https://doi.org/10.5194/egusphere-2025-5531
Preprint. Discussion started: 28 November 2025

New planktonic foraminifera-derived transfer function for the South Atlantic Ocean: Palaeoceanographic implications for the Brazil- Malvinas Confluence

Paula Belén Albarracin[1,2], Natalia García Chapori[1] and Cecilia Laprida[1,2]

[1]Institute of Andean Studies, University of Buenos Aires-CONICET, Argentina

[2]Faculty of Exact and natural Sciences, University of Buenos Aires, Argentina

Correspondence to: Paula B. Albarracin (paula.belen.albarracin@gmail.com) (palbarracin@gl.fcen.uba.ar)

Abstract

Planktonic foraminiferal assemblages are extensively used for reconstructing sea surface temperature through the application of transfer functions. Nonetheless, it has been observed that several parameters present throughout the water column also influence compositional changes within these assemblages. Selection of driving factors and evaluation of transfer function performances are method-specific processes that require the combination of prior ecological knowledge and objective variable selection approaches. In this study, we compiled a 171 core-top samples dataset of planktonic foraminifera and productivity-related variables to quantify the relationship between the assemblages and modern productivity conditions in the South Atlantic Ocean. Multivariate statistical analyses revealed that planktonic foraminiferal species were related to austral summer nitrate, explaining an independent and significant proportion of variance in the species data. We evaluated different prediction models, and estimated their performances considering spatial autocorrelation. The calibration model Weighted Averaging with tolerance downweighting and inverse deshrinking (WATOL_inv) with h-block cross validation showed a regression coefficient of r^2_{cv} = 0.938, with a root-mean-square error of prediction RMSEP = 1.578 umol l^{-1}. The resulting transfer function was applied then to sediment core GeoB2806-4 (~37°S - 53°W; 3500 m) in order to reconstruct variations of summer nitrate concentration during the Holocene. Our reconstructed summer nitrate shows a general decreasing trend from early to mid-Holocene associated with increased biological uptake, and a later increase of it towards the late Holocene. We suggest that changes in summer surface nitrate concentration are linked to the latitudinal shifts of the Brazil-Malvinas Confluence. Understanding the displacement of the Confluence, and the associated shifts in the upper layers' nutrient availability, is crucial to evaluate the implications of these changes on the local to regional ecosystem dynamics and trophic structure, particularly when considering future climate projections.

https://doi.org/10.5194/egusphere-2025-5531
Preprint. Discussion started: 28 November 2025

1. Introduction

Quantitative climate reconstructions are essential for validating climate models' performance when simulating past climate, and thus their potential to predict future climate conditions (Schmidt et al., 2014). Microfossil assemblages derived from marine archives are among the most widely used proxies, providing valuable information about past ocean conditions and climate conditions. These reconstructions build upon the assumption that compositional changes within biotic communities are primarily driven by changes in climatic conditions (Birks et al., 2010).

In this context, transfer functions (Birks, 1995), also known as calibration functions, are one of the most widely applied quantitative approaches. These are multidimensional empirical models that provide a framework for reconstructing past environmental abiotic variables based on the study of fossil biotic components. They have been successfully applied to diverse marine groups, including planktonic foraminifera (e.g., Kucera et al., 2005), diatoms (e.g., Lopes et al., 2018), radiolarians (Hernández-Almeida et al., 2020), and dinoflagellate cysts (e.g., de Vernal et al., 2005). On a more fundamental level, transfer functions approach relies on the assumption that the modern relationship between species abundances and the environmental parameters that define their realized ecological niches is well established and have not changed over time (Birks et al., 2010). By applying multivariate statistical techniques such as multiple regression, ordination, and dimensionality reduction, transfer functions capture and quantify the dominant ecological response patterns expressed in the biological data (Lopes et al., 2010).

Planktonic Foraminifera (Harosa, Rhizaria), are a highly diverse and cosmopolitan group of marine protists (Hemleben et al., 1989). They secrete a calcareous shell with high preservation potential in the fossil record, and their wide geographic distribution, coupled with their sensitivity to specific environmental conditions, render them advantageous proxies. Several transfer functions have been developed using planktonic foraminifera and they have been applied mainly to reconstruct sea surface temperature (SST) (e.g., Imbrie and Kipp, 1971; Hutson and Prell, 1980; Kucera et al., 2005). Nevertheless, the distribution and abundance of the species are not solely governed by SST: many taxa are eurythermic or inhabit deeper layers of the water column (Bé, 1977), making them less sensitive to SST. Moreover, further studies highlighted that species distribution patterns are influenced by multiple interacting environmental factors, including food availability, nutrients, water column stratification, mixed layer depth, sunlight and chlorophyll-a concentration (Bé and Tolderlund, 1971; Berger, 1971; Bijma et al., 1990; Hemleben et al., 1989; Schiebel et al., 2001; Schiebel and Hemleben, 2017; Lessa et al., 2020). Thus, the composition of planktonic foraminiferal communities reflects a combination of processes acting throughout the water column (Morey et al., 2005; Jonkers and Kucera, 2015). Among these variables, nutrient availability regulates the amount of phytoplankton available for consumption, linking bottom-up controls on primary productivity with the trophic dynamics that sustain planktonic foraminiferal communities, and emerging as a key ecological driver at regional scales (Lessa et al., 2020). Collectively, all these environmental parameters mentioned above exhibit seasonal variability driven by hydrographic changes that alter nutrient cycling and marine productivity across the South Atlantic Ocean (Garzoli and Matano, 2011; Muller-Karger et al., 2017). Such dynamics highlight the potential of using biological proxies to capture productivity signals in the geological record.

https://doi.org/10.5194/egusphere-2025-5531
Preprint. Discussion started: 28 November 2025

The South Atlantic Ocean plays a unique role in the global overturning circulation through its equatorward heat transport that modulates climate on decadal time scales (Talley, 2003; Kersalé et al., 2021; Dong et al., 2021). Through the Atlantic Meridional Overturning Circulation, it connects Atlantic water masses with those of others ocean basins (e.g., Garzoli and Matano, 2011). Within this system, two regions of high mesoscale variability in terms of temperature, salinity and primary productivity are developed: the Agulhas Leakage on the eastern boundary, and the Brazil-Malvinas Confluence (BMC) on the western boundary (Jullion et al., 2010; Garzoli and Matano, 2011; Rühs et al., 2019). The former one is shaped by the Benguela Current, which transports a blend of relatively cool, fresh Atlantic water and warmer, saltier Indian Ocean water in a north-westward flow. This current is characterized by recurrent upwelling of cold, nutrient-rich waters along the African coast (Little et al., 1997). In contrast, the western boundary is defined by the BMC, centered near ~38°S (Fig. 1) where warm, salty subtropical waters carried by the Brazil Current converge with cold, nutrient-rich, and relatively fresh subantarctic waters transported by the Malvinas Current (Piola and Matano, 2001). Their confluence forces both currents to turn eastward, flowing offshore in a series of large-scale meanders (Gordon and Greengrove, 1986), and the front itself separates into the Subtropical Front and Subantarctic Front (Fig. 1) (Peterson and Strama, 1991). The BMC is marked by high chlorophyll-a concentrations coinciding with the maximum SST gradient between Malvinas Current and Brazil Current (Saraceno et al., 2004). These highly productive boundary regions interconnect through the South Atlantic Current, the southern limb of the Subtropical Gyre (Stramma and Peterson, 1990). The gyre itself, centered near 30-40°S and 50°W, constitutes a distinct biogeochemical province with notably oligotrophic central waters, hosting some of the lowest chlorophyll-a concentrations observed globally (Longhurst, 2010; Signorini et al., 2015).

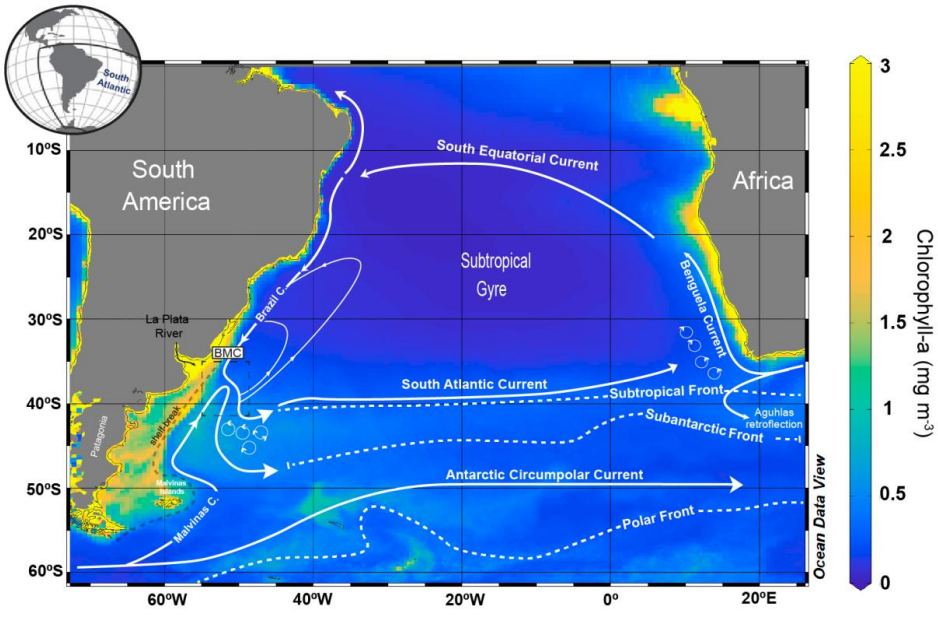

Figure 1: Chlorophyll-a concentration based on data from MODIS Aqua Ocean Color during 2023 (Level-3). Schematic representation of the large-scale surface geostrophic currents and fronts in the South Atlantic Ocean after Peterson and Stramma (1991) are shown. Small loops represent the high concentration of eddies. The mean position of the Subtropical, Subantarctic and Polar fronts is represented with dashed lines. BMC: Brazil-Malvinas Confluence.

https://doi.org/10.5194/egusphere-2025-5531
Preprint. Discussion started: 28 November 2025

Several transfer functions based on planktonic foraminifera assemblages have been developed for the South Atlantic (e.g., Toledo et al., 2007; Pivel et al., 2013; Portilho-Ramos et al., 2015; García Chapori et al., 2015; García Chapori and Laprida, 2021), however, none was explicitly designed to reconstruct past productivity. To fill this gap, in the present contribution we develop a planktonic foraminifera-based transfer function for the quantitative reconstruction of productivity-related variables. With a rigorous statistical analysis of the relationship between assemblage data and these variables, we identify the primary factors that determine species distributions and abundances within the calibration dataset. To improve the spatial coverage of the BMC region, we incorporated new samples into the calibration dataset. We then calibrate and evaluate several transfer functions models for predicting the selected environmental variables and asses their performances. The obtained transfer function is used to reconstruct past primary productivity changes in the BMC influence zone during the Holocene. The results obtained are compared with regional reconstructions of mixed-layer temperature and inferred BMC shifts from independent proxies in order to contextualize primary productivity changes within a paleoceanographic framework.

2. Materials and methods

2.1 Calibration dataset

2.1.1 Surface samples

Geographic distribution of planktonic foraminiferal species was assessed through the analysis of a bunch of 358 surface sediment samples (core-tops) from the South Atlantic Ocean. These samples spanned the first 5 cm and hence they were assumed to represent present-day conditions. In order to avoid the problem of the lack of analogs, while covering the entire productivity environmental gradients, we consider the Euclidean distance to explore the multivariate structure of the species' abundance data. For the selection process, 335 core-tops from the compilation of Siccha and Kucera (2017), 11 core-tops from the compilation of García Chapori and Kucera (2019) and 12 new core-tops collected from the Argentine and Uruguay margins between 36°S - 39°S (Cruise SO260 "DosProBio"; Kasten et al., 2019) were analyzed.

2.1.2 Selected environmental variables

Phosphate, nitrate, silicate, chlorophyll-a and iron were interpolated to the core-tops' locations using Ocean Data View (ODV) software (Schlitzer, 2014). Phosphate, nitrate, and silicate from the upper 10 m of the water column were obtained from the 2013 World Ocean Atlas (WOA13 – García et al., 2014), based on a grid of 1° longitude by 1° latitude. Chlorophyll-a and iron data were obtained from MODIS-aqua (http://oceancolor.gsfc.nasa.gov/l3.) and the NASA Ocean Biogeochemical Model (NOBM) (Gregg et al., 2003) respectively. Iron data were calculated from measurements between 1998 and 2012 with a 0.67 x 1.25° resolution, whereas chlorophyll-a data was structured on a basis of 4 km of spatial resolution and covers measurements between 2002 and 2012. For each variable, we calculated austral seasonal means: summer (DJF); autumn (MAM); winter (JJA) and spring (SON) from 1955 to 2012 resulting in a total of 20 productivity-related variables. The temporal ranges selection was based on the fact that measurements from recent years are influenced by global warming (Forster et al., 2023).

https://doi.org/10.5194/egusphere-2025-5531
Preprint. Discussion started: 28 November 2025

Therefore, we analyzed seasonal averages, considering the complex and highly dynamic regions included in the calibration dataset. These areas are subjected to seasonal cycles in their physical oceanography (SST, vertical stratification, thermal and haline fronts, upwelling systems, and current patterns), which in turn regulate their biological productivity regimes (Dave et al., 2015; Artana et al., 2019; Gallego et al., 2025).

2.2 Sediment core

Sediment core GeoB2806-4 (37°50'S - 53°08.6'W, 3500 m depth; García Chapori et al., 2015) was used for testing the transfer function developed here. The core is located on the northern Argentine continental margin, within the BMC zone (Fig. 2). The selected core is optimally located and guarantees excellent modern analogues in the fossil assemblages (García and Laprida, 2021). The core spans the last 12 kyrs BP, covering the entire Holocene. The radiocarbon-based chronology was previously developed by García Chapori et al. (2015). Here we updated the age model using the original radiocarbon dates and additional benthic $\delta^{18}O$ data (Fig.S1 in the Supplement), and applying the Bayesian software package BIGMACS (Lee et al., 2023). We integrated the results obtained here with other reconstructions performed for the region (i.e., García Chapori et al., 2022); particularly the annual mixed-layer temperatures obtained by García Chapori and Laprida (2021) for this same core, and analyzed the existent relationship between productivity and temperature changes.

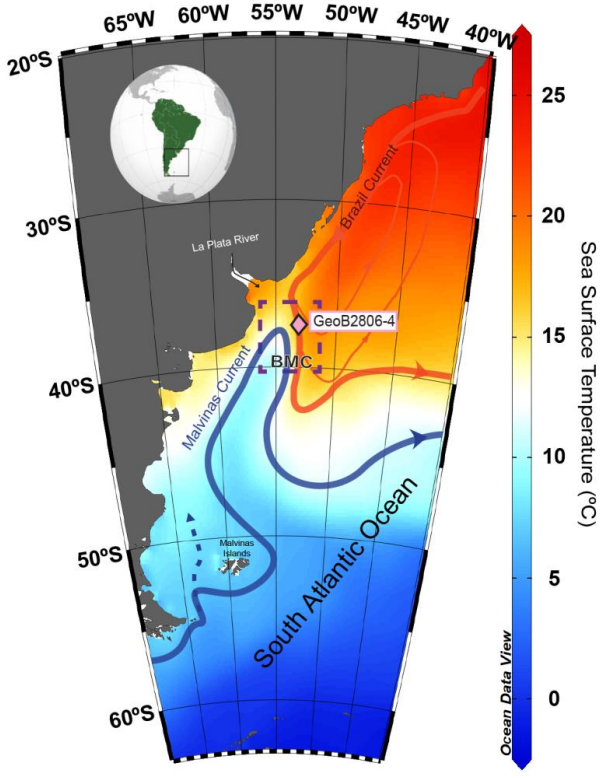

https://doi.org/10.5194/egusphere-2025-5531
Preprint. Discussion started: 28 November 2025

Figure 2: Mean annual SST (color, °C) from World Ocean Atlas, 2013 with scheme of major oceanic currents from the western South Atlantic. Sediment core GeoB2806-4 location is represented by a pink diamond. BMC: Brazil-Malvinas Confluence.

2.3 Micropaleontological analyses

Samples were prepared for foraminiferal analyses according to the micropaleontological techniques proposed by Boltovskoy and Wright (1976). Planktonic foraminifera were dry picked from the >150 µm size fraction (Kucera et al., 2005) and quantified in relative abundances from splits containing at least 300 specimens per sample. We harmonized the taxonomic nomenclature following the criteria established by Siccha and Kucera (2017). In cases where the original taxonomy required the grouping of species, and to harmonize the possible taxonomic differences between assemblages, these categories were retained as multispecies categories (groups) (Jonkers et al., 2025). These criteria were applied to the group of menardiforms (*Globorotalia menardii* + *Globorotalia tumida* + *Globorotalia ungulata*), which were included into the "*G. menardii* complex" group, and to the morphotypes white and pink of *Globigerinoides ruber*, which were included within the "*G. ruber* (total)" group. Species with <2% abundance in at least two samples were removed from the dataset prior to further analysis (Fatela and Taborda, 2002). Percentage foraminiferal census data were log-transformed (log (x+1)) in order to standardize their variances.

2.4 Multivariate analyses

A principal component analysis (PCA), with variables scaled to unit environmental variance and centered, was used to explore the main gradients in the environmental data according to their geographical location. The 'broken stick' model was used to assess the significance of the PCA axes (Jackson, 1993). To examine the local relationship between planktonic foraminiferal assemblages and environmental variables, a detrended correspondence analysis (DCA) was performed (Birks, 1995), measuring the gradient length in standard deviation (SD) units along the first DCA axis. Consequently, we determined whether linear ordination techniques (SD<3) or unimodal techniques (SD>4; Lepš and Šmilauer, 2003) should be applied. As the dataset was found to have a SD of 2.6 using log-transformed foraminiferal assemblage, we opted for linear statistical ordination techniques.

To explore the relationships between the species variance and the 20 selected environmental variables, we employed a Redundancy Analysis (RDA), a constrained ordination technique suitable for linear datasets (McGarigal et al., 2000). First, a RDA was performed individually for each environmental variable to obtain their eigenvalues, which were then ranked based on their contribution to the dataset variance. Monte Carlo permutation tests were applied to evaluate the statistical significance of these relationships (ter Braak and Smilauer, 2002). Second, we identified the variable with the highest eigenvalue and systematically added the other variables based on their rank. To assess potential collinearity among these variables, we calculated Variance Inflation Factors (VIFs), which indicate how much of the variance explained by one environmental variable is already accounted for another variable in the dataset. To ensure minimal collinearity, a VIF threshold of ≤2 was established for all environmental variables in line with prior research recommendations (e.g., Lopes et al., 2010). This threshold limits collinearity to correlations $r^2 \leq 0.5$, ensuring

https://doi.org/10.5194/egusphere-2025-5531
Preprint. Discussion started: 28 November 2025

that no more than half of one variable's explained variance can also be attributed to another variable. While using a lower VIF cut-off helps retain critical environmental factors in our model, it may also prevent the inclusion of collinear variables that could negatively impact on the model quality. By adopting this cautious methodology, we aimed to identify as many independent variables as possible while still accounting for significant variance in our dataset.

In order to test the significance of each variable, we implemented a manual forward selection process that ranked variables according to their ability to explain data variance (Manly, 1991; ter Braak, 1992; ter Braak and Verdonschot, 1995). During this procedure, any environmental variables with VIFs > 2 were excluded from the analysis. In instances where multiple variables had VIFs above this threshold, we iteratively removed one variable at a time and conducted RDAs on each remaining subset of data. This iterative approach enabled us to quantify how much variation was accounted for by different variables within the dataset and ultimately identify a final set of variables that maximized the overall explained variance. As a result of this process, we established a set of environmental variables appropriate for use in our calibration datasets during subsequent RDAs and additional analyses. We used the ratio between constrained (λ_1) and unconstrained (λ_2) axes as diagnostic tools to assess individual environmental variable strength after excluding the effects of the other variables from the analysis (ter Braak and Juggins, 1993). Values of $\lambda_1/\lambda_2 \geq 1$ were considered an indicator of how well the variable under examination is strongly related to the variation in the modern foraminifera dataset. Ordination analyses and variance partitioning were performed using CANOCO version 5.03 software (ter Braak and Smilauer, 2002).

After assessing which environmental variables could theoretically be reconstructed, we examined spatial and environmental autocorrelation following the procedure described by Telford and Birks (2009). We applied the Modern Analog Technique (MAT) with five analogues as part of our reconstruction testing approach. To ensure an accurate transfer function evaluation, we determined the extent of autocorrelation which requires spatial independence among sample sites (Telford and Birks, 2009). For this analysis, we used R packages fields (Nychka et al., 2017), palaeoSig (Telford, 2015) and rioja (Juggins, 2017).

2.5 Transfer function

In order to establish the transfer function, five different calibration models were evaluated: Modern Analogue Technique (weighted average of the five closest analogs) (WMAT) (Prell, 1985), Weighted Averaging (WA) developed by Birks et al. (1990), Weighting-Averaging Partial Least Squares (WA-PLS) (ter Braak & Juggins, 1993) and Maximum Likelihood (ML) as described by Oksanen et al. (1990). The WA model was evaluated concerning tolerance downweighting (referred to as WA-TOL), along with classical (WA- Cla) and inverse deshrinking methods (WA- inv); whereas the WA-PLS model was assessed based on the number of components utilized (ter Braak & Juggins, 1993). The number of components for the WA-PLS model was chosen by the improvement in the RMSEP >5% (Birks, 1998) and the significance derived from randomization t-test conducted on each model. The 'best' performance of each model was determined by the highest r^2 value and lowest RMSEP, all assessed by cross validation (999 permutation cycles) (Birks, 1995). Additionally, the average and maximum bias for each model was also considered. Potential outliers were identified based on the evaluation of the absolute residuals. Sites with residuals larger than 4 were finally removed as outliers. These analyses were done using C2 software version 1.4.3 (Juggins, 2007).

https://doi.org/10.5194/egusphere-2025-5531
Preprint. Discussion started: 28 November 2025

A common issue when evaluating the selected model using cross-validation is that calibration and validation data selected randomly from proximate locations may exhibit spatial dependency due to autocorrelation. This can result in an underestimation of prediction errors; potentially misleading the model selection (Roberts et al., 2017). To address these spatial dependencies within our dataset, we adopted the h-block method (Burman et al., 1994), which excludes samples situated closer than a specified cut-off distance (h) from contributing to the prediction of that target sample. The cut-off distance was determined by fitting a spherical variogram to detrended residuals of a WA model before conducting h-block cross-validation utilizing R packages gstat (Pebesma, 2004) and sp. (Pebesma and Bivand, 2005), R code developed by Trachsel and Telford (2016).

3. Results

3.1 Geographical distribution of planktonic foraminiferal assemblages in the calibration dataset

The final calibration dataset used in this study comprises 171 core-tops (Fig. 3), encompassing the whole primary productivity gradient across the South Atlantic Ocean. The taxonomic homogenization resulted in a matrix with 29 taxonomic categories. The distribution pattern of the relative abundance of the main planktonic foraminifera taxa (≥10%) are shown in Figure 4.

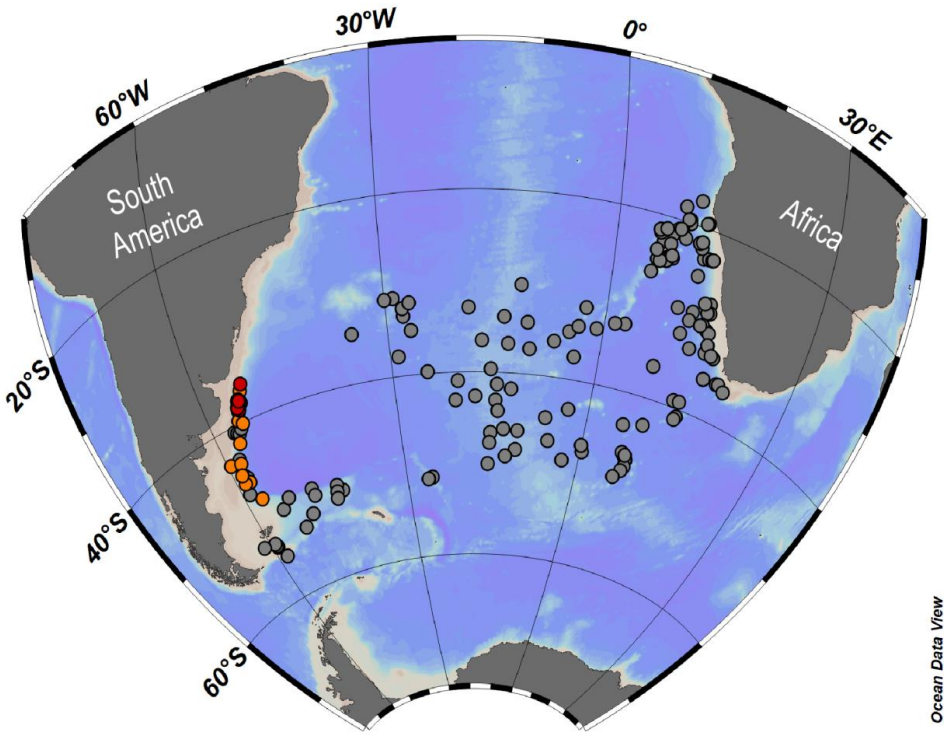

Figure 3. Location of the 171 core-top samples used for the compilation of the calibration dataset after the Euclidean distance analysis. Red circles represent new core tops from this study, orange circles correspond to core tops from the

https://doi.org/10.5194/egusphere-2025-5531
Preprint. Discussion started: 28 November 2025

compilation of García Chapori and Kucera (2019), and grey circles indicate core tops from the compilation of Siccha and Kucera (2017).

In the calibration dataset, *Globigerina bulloides* (Fig.4a) is the most common species, constituting up to 60% of the assemblage in the transitional zone between the Subantactic Front and the Subtropical Front, while it has its lowest abundance (1 %) within the South Atlantic Current. In upwelling systems like the Patagonia shelf-break and Benguela (Romero et al., 2006; Petrick et al., 2015), its mean relative abundances is ~35%. *Neogloboquadrina pachyderma* (Fig.4b) exhibits maximum relative abundances (up to 80%) along the Polar Front (south of 50°S), with abundances below 15% north of 45°S and minima abundance in the South Atlantic Current and Benguela system. *Globoconella inflata* (Fig. 4c) exhibits high relative abundances (mean 48%) within the BMC region and reaches values of up to 23% along the Patagonian shelf-break. Toward the eastern margin of the calibration dataset, this species achieve abundances close to 50% in some areas of the Benguela region. In contrast, it is not a common species in the Subantactic and Polar fronts, where it shows minimal abundances. *Neogloboquadrina incompta* (Fig. 4d) reaches its highest relative abundances within the Benguela system and the South Atlantic Current region (up to ~42%), and occurs with ~25% abundance along the Patagonian shelf break. In contrast, *N. incompta* is a scarce component of the assemblages in the Subantarctic and Polar Front regions. *Neogloboquadrina dutertrei* (Fig. 4e) dominates most of the eastern sector of the calibration dataset, reaching abundances up to 40% within the Benguela system. *Globigerina falconensis* (Fig. 4f) reaches its highest abundances along the South Atlantic Current (up to 35%) and is rare in the western South Atlantic, across the Polar Front, and north of 30°S in the calibration dataset. *Globigerinoides ruber* (total) (Fig. 4g) shows maximum relative abundances of up to 30% along the South Atlantic Current; however, south of 40°S, its abundance decreases sharply to below 1%. *Orbulina universa* (Fig. 4h) attains its highest abundances exclusively north of the Benguela system while *Globigerinita glutinata* (Fig. 4i) displays patchy distribution with high-abundances across Benguela, the Agulhas Retroflection, and the South Atlantic Current. Finally, *Globorotalia truncatulinoides* (Fig. 4j) achieves its highest abundances (~12%) between 30° and 40°S within the calibration dataset, including the South Atlantic Current region. In contrast, it is much less abundant in the Benguela system and becomes virtually absent south of the Polar Front (>50°S).

https://doi.org/10.5194/egusphere-2025-5531
Preprint. Discussion started: 28 November 2025

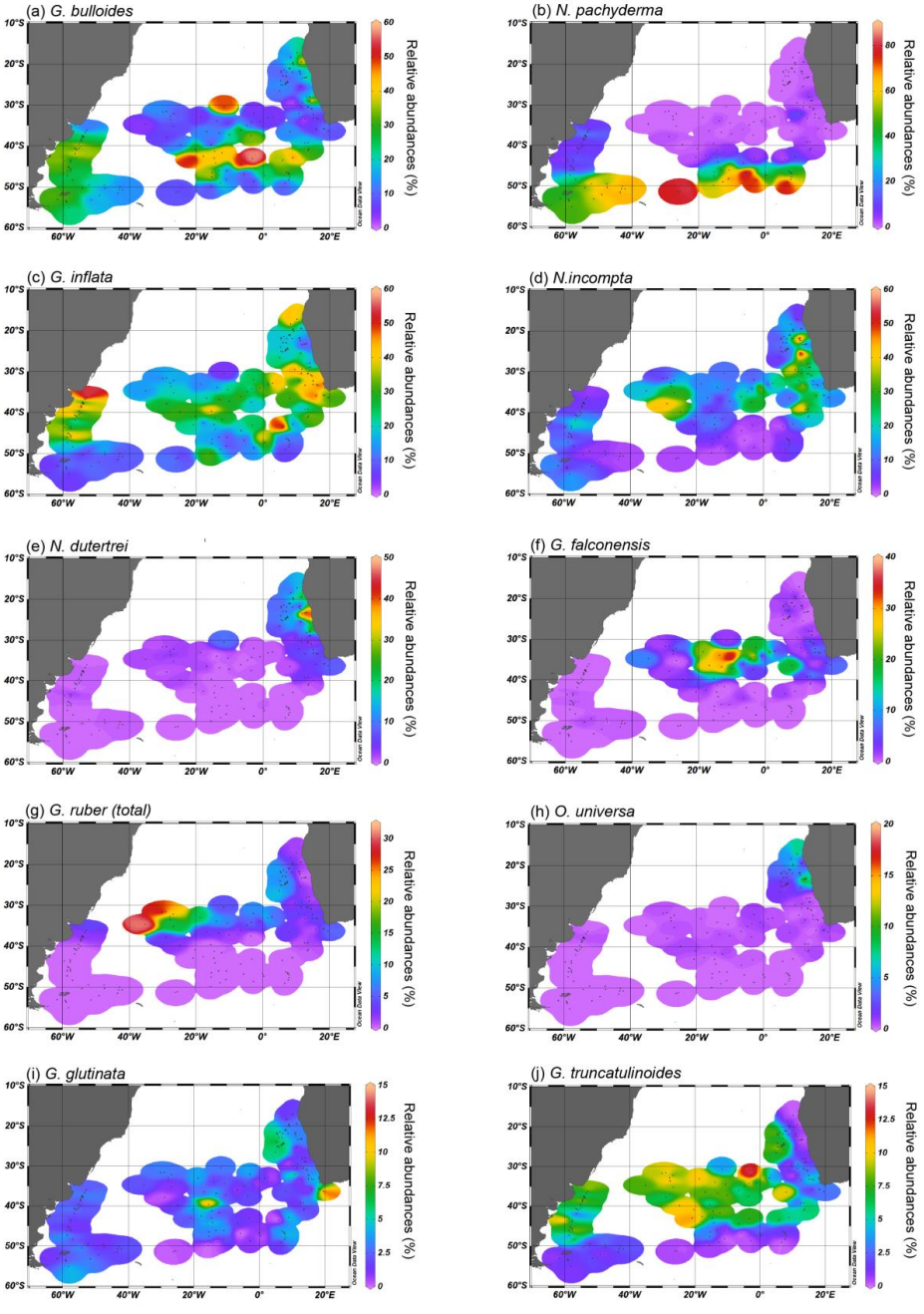

Figure 4: Geographical distribution of the main planktonic foraminifera taxa according to their relative abundance (%), Panel (a) *Globigerina bulloides*, (b) *Neogloboquadrina pachyderma*, (c) *Globoconella inflata*, (d) *Neogloboquadrina incompta*, (e) *Neogloboquadrina dutertrei*, (f) *Globigerina falconensis*, (g) *Globigerinoides ruber* (total), (h) *Orbulina universa*, (i) *Globigerinita glutinata* and (j) *Globorotalia truncatulinoides*.

https://doi.org/10.5194/egusphere-2025-5531
Preprint. Discussion started: 28 November 2025

3.2 Dimensionality of the Environmental Data

The 20 candidate environmental variables are highly collinear. The first two PCA axes explain 76.9% of the total variance in the calibration dataset, being both significant according to the broken stick model (Fig. S2 in the Supplement). PCA1 explains 47.2% of the variance, and it is positively correlated with phosphate and nitrate across all seasons, as well as spring and winter silicate. PCA2 explains 29.7% of the variance and it is correlated with chlorophyll-a and iron concentrations (Fig. 5a).

The spatial distribution of the samples combined with their PCA scores allowed the identification of three distinct groups in the environmental dataset: the Central South Atlantic (CSA), the Eastern South Atlantic (ESA) and the Western South Atlantic (WSA) (Fig. 5b). Therefore, when analyze the biplot of the first two PCA components, it shows that all samples from the CSA group contribute to the variance in the PCA1 axis. Instead, samples from the ESA group contribute to the variance in the both axes, PCA1 and PCA2, while the WSA group evidences a clear separation between samples (Fig. 5a). At a more detailed level, two distinct subregions can be distinguished along a latitudinal gradient: north WSA (north of 45°S) samples showed a striking correlation with PCA2 axis suggesting that the variance of chlorophyll-a and iron is high in this subregion. Instead, south WSA (south of 45°S) samples were positively correlated with PCA1 components, showing a similar sample-environment relationship with the CSA region.

https://doi.org/10.5194/egusphere-2025-5531
Preprint. Discussion started: 28 November 2025

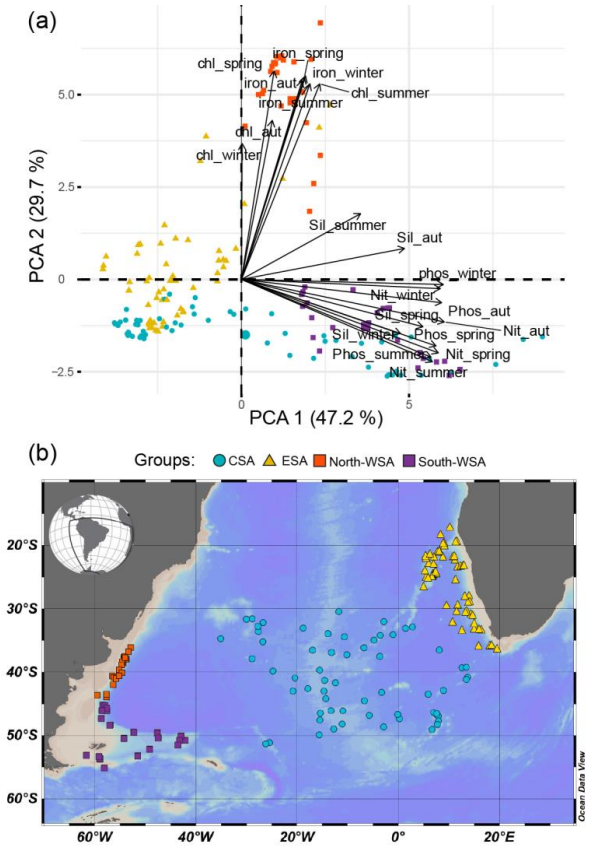

Figure 5: (a) Principal Component Analysis (PCA) biplot of the seasonal (summer, autumn, spring, winter) surface environmental variables. Nit: nitrate; Phos: phosphate; Sil: silicate; chl: chlorophyll-a; iron. Yellow triangles correspond to samples located on the Eastern South Atlantic (ESA); blue circles correspond to samples located on the Central South Atlantic (CSA); red squares to samples located north of 45° S on the Western South Atlantic (North-WSA); and purple squares to samples located south of 45° S on the Western South Atlantic (South-WSA). (b) Geographical distribution of the calibration dataset samples where the ESA (yellow triangles), CSA (blue circles), North-WSA (red squares) and South-WSA (purple squares) are distinguished.

3.3 Foraminiferal assemblages – environment relationship

The RDA results revealed that, when considered individually, ten of the twenty environmental variables appeared to explain a significant ($p \leq 0.001$) amount of variation in the assemblage composition of the dataset (Table 1). However together, these explain 57.7 % of the total inertia. Therefore, we evaluated the variables' independence excluding those with VIF >2. The successive forward selection revealed that only surface Nitrate_summer, Silicate_summer and Chl_autumn explained a significant amount of variance within the assemblages. These three environmental variables together explain 44.6% of the total variance, being Nitrate_summer the variable that explained the highest proportion of variance (considering simple and conditional effects) (Table 2). The first RDA axis explains 40.27 % of the constrained variance and is positively correlated with Nitrate_summer and

https://doi.org/10.5194/egusphere-2025-5531
Preprint. Discussion started: 28 November 2025

Silicate_summer (Fig. 6a), while the second RDA axis explains 4.33% and is positively correlated with Chl_autumn (Fig. 6a). The individual RDA λ_1/λ_2 (Table 3) showed that surface Nitrate_summer was the most important variable among those found to be significant suggesting it represents an important ecological gradient in the calibration dataset (Juggins, 2013).

Table 1: Explained inertia of the tested environmental variables in the RDA model when all variables are considered.

Enviromental variable	% inertia explained	Contribution %	pseudo-F	p value
Nitrate_summer	**39.8**	**61.4**	**112**	**0.001**
Nitrate_autumn	**3.2**	**4.9**	**9.8**	**0.001**
Nitrate_spring	**3**	**4.7**	**8.9**	**0.001**
Nitrate_winter	**2.2**	**3.4**	**7.4**	**0.001**
chl_summer	**2.2**	**3.4**	**8.5**	**0.001**
Silicate_spring	**1.8**	**2.8**	**6.3**	**0.001**
chl_aut	**1.7**	**2.6**	**7.3**	**0.001**
iron_summer	**1.4**	**2.1**	**5.3**	**0.001**
phos_summer	**1.2**	**1.8**	**3.7**	**0.001**
iron_spring	**1.2**	**1.9**	**5.1**	**0.001**
chl_winter	1.4	2.2	5.1	0.002
phos_winter	1.3	1.9	4.1	0.002
iron_winter	1.1	1.6	4.3	0.002
phos_spring	0.9	1.4	2.7	0.017
phos_winter	0.9	1.4	2.8	0.019
Silicate_winter	0.6	0.9	2.2	0.047
Silicate_summer	0.5	0.8	1.9	0.096
Silicate_autumn	0.3	0.5	1.3	0.216
iron_autumn	0.2	0.3	0.7	0.593
chl_spring	<0.1	<0.1	0.3	0.94

Table 2: Results of Redundancy Analysis (RDA) for planktonic foraminifera species abundance based on core-top samples and variables explaining a significant amount of variance with (a) simple effects and (b) conditional effects.

Statistic	Axis 1	Axis 2	Axis 3	Axis 4
Eigenvalues	0.4027	0.0433	0.0021	0.1596
Explained variation (cumulative)	40.27	44.6	44.82	60.78
Pseudo-canonical correlation	0.9189	0.6113	0.1763	0
Explained fitted variation (cumulative)	89.86	99.53	100	

(a) Simple Term Effects:				
Enviromental variable	Explains %	pseudo-F	P	P(adj)
Nitrate_summer	39.8	112	0.001	0.003
Silicate_summer	6.3	11.4	0.001	0.003

https://doi.org/10.5194/egusphere-2025-5531
Preprint. Discussion started: 28 November 2025

chl_autumn	4.6	8.2	0.001	0.003

(b) Conditional Term Effects:				
Enviromental variable	Explains %	pseudo-F	P	P(adj)
Nitrate_summer	39.8	112	0.001	0.003
chl_autumn	4.3	12.8	0.001	0.003
Silicate_summer	0.7	2.2	0.057	0.171

Table 3: Explained inertia and variance inflation factors (VIF) of the tested environmental variables in the after manual forward selection for variables without redundancy.

Enviromental variable	% inertia explained [RDA]	VIF	λ_1/λ_2
Nitrate_summer	39.8	1.13	2.35
Silicate_summer	6.3	1.14	0.10
chl_autumn	4.6	1.05	0.06

Based on RDA axis ordination, four different environmental settings can be characterized (Fig. 6a). Quadrant I represents a biological state characterized by high chlorophyll-a concentrations in autumn (Chl_autumn), indicative of enhanced productivity. Quadrant II corresponds to nutrients/production state associated with summer nutrients (nitrate and silicate) together with Chl_autumn production. Quadrant III represents low-productivity environments, characterized by reduced chlorophyll-a and depleted nutrient levels and quadrant IV represents nutrient-driven conditions with low chlorophyll-a (Fig. 6a). Regarding planktonic foraminifera species distribution, the 'environmental quadrants' revealed that polar species were more associated with high values of summer nitrate and silicate (Fig. 6a). *Neogloboquadrina dutertrei*, *Orbulina universa* and *Globoconella inflata* were associated with quadrant I, while *Globigerina bulloides* was linked with quadrant II. In quadrant III, species such as *Neogloboquadrina incompta*, *Globorotalia truncatulinoides*, *Globigerinita glutinata*, *Globorotalia hirsuta*, *Globigerinoides tenellus*, *Globigerinella calida*, *Globigerinella siphonifera*, *Trilobatus sacculifer*, *Globigerinoides conglobatus*, "*G. menardii complex"*, and the "*G. ruber* total" were present, except for *Globigerinita uvula* and *Berggrenia pumilio*, which were closer to the axes' origin. *Neogloboquadrina pachyderma* and T*urborotalita. quinqueloba* showed their optimal conditions in quadrant IV. Sample–environment relationships (Fig. 6b) indicate that samples from the WSA and CSA regions contribute to the variance in surface Nitrate_summer and Silicate_summer, whereas chlorophyll-a variance is mainly explained by samples from both the ESA and WSA.

https://doi.org/10.5194/egusphere-2025-5531
Preprint. Discussion started: 28 November 2025

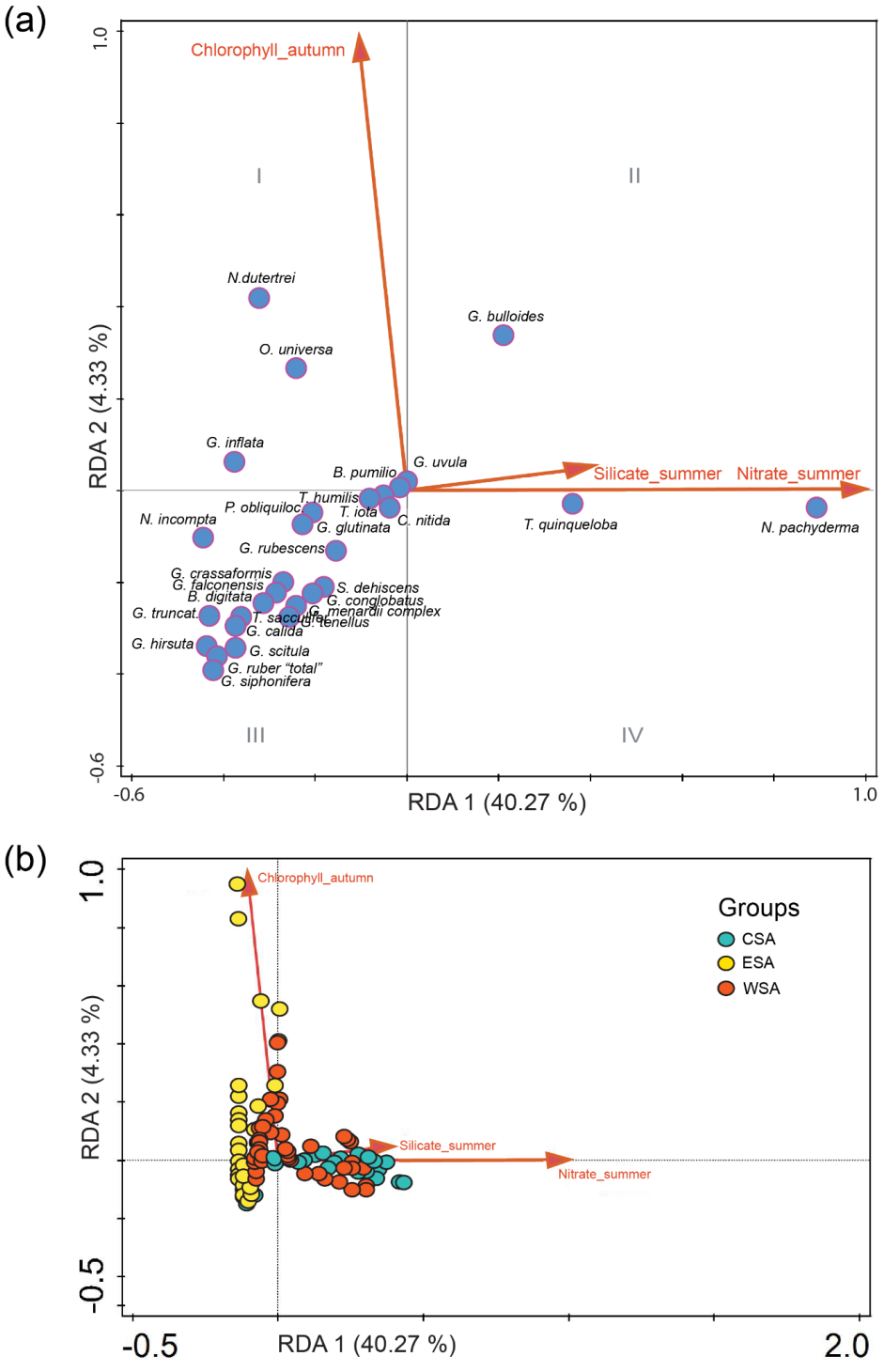

https://doi.org/10.5194/egusphere-2025-5531
Preprint. Discussion started: 28 November 2025

Figure 6: (a) RDA ordination diagrams illustrating the selected planktonic foraminiferal species, constrained by independent environmental variables from the calibration dataset. The environmental variables (represented by red arrows) indicate their correlation with the axes (the direction of arrows) and their significance in explaining the distribution of planktonic foraminifera (the length of arrows). (b) Sample ordination for RDA, constrained by independent environmental variables for RDA 1 and 2 within the calibration dataset.

3.4 Transfer Function Selection

Surface Nitrate_summer explained the largest amount of variation in the planktonic foraminifera assemblages and was therefore chosen to develop the transfer function. Twenty-one samples were identified as outliers and removed from the calibration dataset. Performance statistics for the twelve evaluated transfer function models are shown in Table 4. The bootstrap cross-validation shows that WATOL_inv performs the best model, achieving the highest cross-validated coefficient of determination, as well as the lowest RMSEP. The other models had slightly worse performances, with lower r^2 values and higher RMSEP (Table 4).

Table 4: Performance statistics for all transfer function models for Nitrate_summer based on bootstrap cross validation method after removal of outliers.

Model	r^2 (boot)	RMSEP	Average bias (boot)	Maximum bias (boot)
MAT	0.929	1.729	-0.071	5.502
WMAT	0.934	1.663	-0.085	5.666
WA-PLS1	0.916	1.775	0.007	2.614
WA-PLS2	0.921	1.737	0.016	2.686
WA-PLS3	0.919	1.771	0.001	2.673
WA-PLS4	0.917	1.821	-0.001	2.576
WA-PLS5	0.916	1.868	-0.013	2.610
WA_Inv	0.916	1.778	0.003	2.608
WA_Cla	0.916	1.846	0.000	3.409
WATOL_Inv	**0.942**	**1.550**	0.142	3.341
WATOL_Cla	0.942	1.560	0.146	2.718
ML	0.936	1.610	-0.247	3.509

After assessing which environmental variables could theoretically be reconstructed, we tested for the presence of spatial and environmental autocorrelation. The results indicate that the performance (r^2) of the MAT deteriorates with increasing fraction of sites deleted (Fig. 7). For instance, removing sites within a 500 km neighborhood of each site results in an average decrease of only 10% in the number of available analogues, but the performance of Nitrate_summer reconstruction deteriorates from $r^2 = 0.876$ to 0.781. In contrast, achieving a similar decline in performance through random site deletion requires the removal of 70% of available sites (Fig. 7). This demonstrates that the deletion of nearby sites is not equivalent to the deletion of sites at random, suggesting the presence of spatial autocorrelation. On the other hand, when environmentally similar sites are deleted, we observe that the performance loss is more pronounced with neighborhood deletion compared to environmental deletion (Fig. 7). Due to the observed autocorrelation, we employed the second method suggested by Trachsel and Telford (2016). The estimated range of a circular variogram model fitted to the detrended residuals of the weighted average

https://doi.org/10.5194/egusphere-2025-5531
Preprint. Discussion started: 28 November 2025

model is 868 km. This result indicates that samples within a distance h of 868 km may be considered potentially identical and should be excluded during h-block cross-validation to avoid over- optimistic estimates. Therefore, we repeated the calibration model including a cut-off value for h-block cross validation to obtain unbiased performances. Results from each model with bootstrap and h-block cross validation are shown in Table 5. An inspection of the residual distribution from the cross-validation tests (both bootstrapped and h-block), however, reveals uneven residual patterns for Nitrate_summer (Fig.S3 in the Supplement). For the two models considered, the spatial structure of the residuals is complex and large residual values emerge at different regions. In the case of bootstrapped cross-validation, large over- and underestimations were observed across a substantial portion of the calibration dataset. However, when using h-block cross-validation, the largest overestimations were concentrated south of 45°S and north of 20ºS, while residuals remained relatively small along a broad latitudinal band between 20°S and 45°S. Despite presenting slightly lower performance and higher RMSEP, we adopted the h-block approach because it explicitly corrects for spatial autocorrelation, preventing the artificial inflation of the model performance. This outcome highlights that the h-block approach is the most effective for evaluating model performance and further indicates that the transfer function provides its most reliable reconstructions within this latitudinal range.

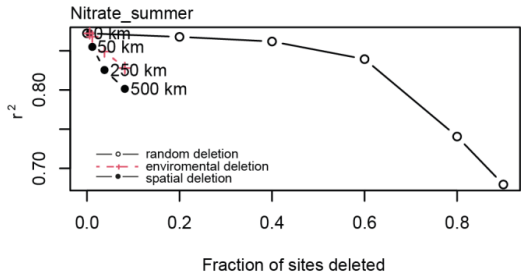

Figure 7: Effect of random site deletion, neighborhood deletion (testing four distances) and environmental deletion on the performance of the Nitrate_summer transfer function, expressed as the r^2 between observed and predicted values.

Table 5: Performance statistics for each calibration model. Coefficients of determination (r^2) and root mean square error of prediction (RMSEP) assessed with bootstrap and h-block cross validation methods.

Model	Cross validation	$R^2_{(cv)}$	RMSEP
WATOL_Inv	bootstrapped	0.941	1.561
	h-block	**0.938**	**1.578**

The surface Nitrate_summer values in the calibration dataset vary from 0.148 to 21.20 µmol l^{-1} (Fig. 8a). WATOL_inv predicted values are shown in Figure 8b. The predicted *vs*. observed values approach the diagonal of slope one (which indicates perfect predictions) reasonably well (Fig. 8c). The residuals are equally distributed around zero and do not exhibit any apparent trends (Fig. 8d). Based on these results, we suggest that the WATOL_inv model offers the most robust and unbiased reconstruction for surface Nitrate_summer, making it the most reliable calibration tool for paleoproductivity reconstructions in the South Atlantic Ocean.

https://doi.org/10.5194/egusphere-2025-5531
Preprint. Discussion started: 28 November 2025

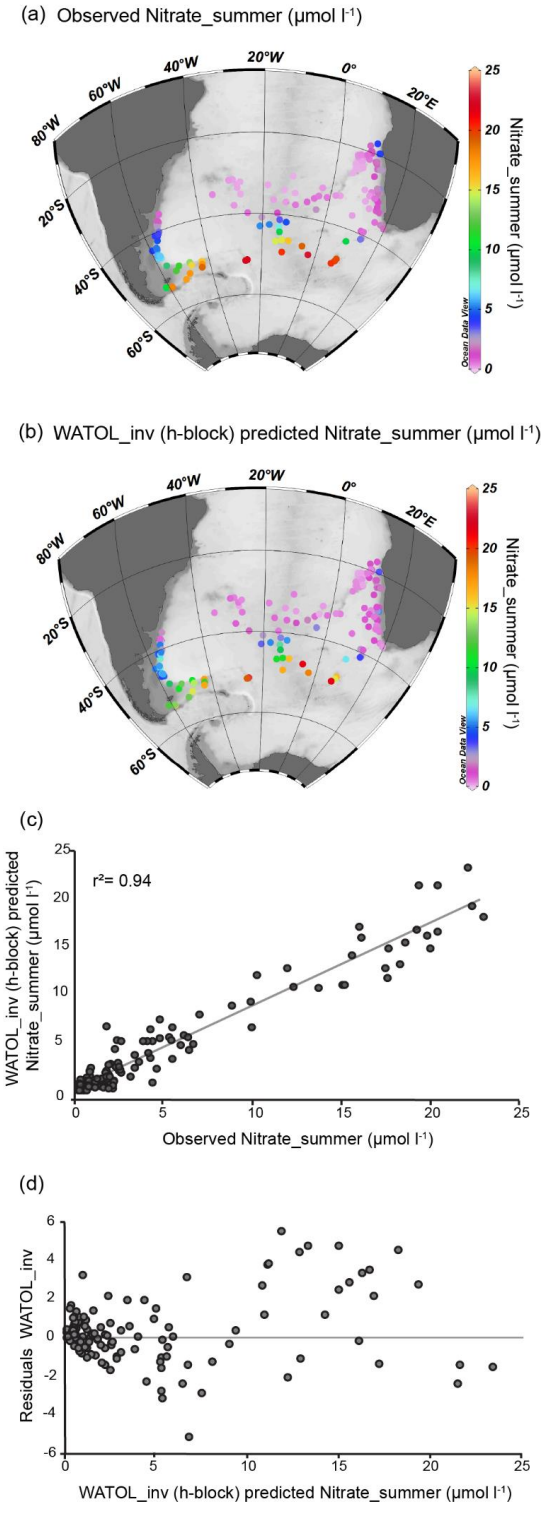

https://doi.org/10.5194/egusphere-2025-5531
Preprint. Discussion started: 28 November 2025

Figure 8: Diagnostic plots of the South Atlantic transfer function. (a) Observed Nitrate_summer values; (b) WATOL_inv-predicted h-block cross-validation Nitrate_summer values (without outliers); (c) Observed vs. WATOL_inv-predicted h-block cross-validation Nitrate_summer values (without outliers) (d); WATOL_inv-predicted h-block cross-validation Nitrate_summer values vs. residuals (without outliers).

4. Discussion

The calibration dataset constrained here spans a broad latitudinal gradient that encompasses key oceanographic features such as the subtropical gyre, the confluence of two major western boundary currents, several frontal systems, upwelling regions, and mesoscale eddies. Nutrient-related environmental gradients independently contribute to explain the geographic distribution of planktonic foraminiferal assemblages in the South Atlantic. Lessa et al. (2020) suggested that primary productivity can dominate the assemblage composition within the mixed layer while physical factors such as temperature and salinity become more significant at intermediate and subsurface depths. Some planktonic foraminifera species occupy a narrow ecological niche, and flourishes at places and during times of slightly enhanced nutrient availability following the phytoplankton production (Schiebel and Hemleben, 2017). Many euphotic-zone-dwelling foraminifera almost certainly discriminate in the forms of the N they consume, perhaps preferentially consuming zooplankton as well as larger phytoplankton (Bé and Hutson, 1977; Spindler et al., 1984). In contrast, the deeper-dwelling, non-spinose foraminifera species appear to feed more passively and thus less selectively. The finding that productivity-related variables influence the abundance of planktonic foraminiferal species in surface sediments is not unexpected. What is distinctive and novel is the identification of surface Nitrate_summer as the principal driver in the South Atlantic. However, our knowledge of how nitrate availability affects planktonic foraminiferal distribution remains limited.

4.1 Modern calibration dataset

Designing a robust planktonic foraminifera dataset is a critical part of a paleoenvironmental reconstruction process as the reconstructed values strongly depend on the empirical relationships between the modern distribution and abundance of taxa, and the modern environmental measurements (Kucera et al., 2005). The accuracy and reliability of any reconstruction depends on the span (i.e., the width of the environmental gradient covered by the sampled sites), the size (i.e., the number of data points), and the coverage of the environmental gradient (i.e., the distribution of the samples along that gradient) (Juggins and Birks, 2012). The size of our calibration dataset, and the distribution of our samples along the studied productivity gradient accurately capture the regional planktonic foraminifera-environmental relationships in the South Atlantic. Our results highlight three distinctive regions: the WSA, the ESA and the CSA regions (Fig. 5).

Nowadays, the WSA is recognized as a key region in the global carbon cycle, functioning as a significant sink for atmospheric CO_2 via both the biological and solubility pumps (Field et al., 1998; Sigman et al., 2010). Our findings indicate that the productivity gradient within the WSA presents a north-south orientation shaped by multiple interacting variables. This pattern led to the characterization of two subregions: the northern WSA and the southern WSA (Fig. 5b). Northern WSA (north of 45°S) is strongly influenced by the BMC itself, where high chlorophyll-a concentrations can be recognized (García et al., 2004; Saraceno et al., 2005; Barré et al., 2006). This high productivity arises from the optimal interplay between the nutrient-rich subantarctic waters advected by the

https://doi.org/10.5194/egusphere-2025-5531
Preprint. Discussion started: 28 November 2025

Malvinas Current and the warm subtropical waters of the Brazil Current, a combination that generates ideal conditions for enhanced primary production and efficient photosynthetic carbon uptake. This part of the margin is additionally affected by other sources of nutrients such as the freshwater discharges from the Río de la Plata (~36°S) and Lagoa Dos Patos (~32°S), which provide a substantial input of terrestrial material (Brandhorst and Castello, 1971; Depetris and Paolini, 1991). Combined with wind forcing, these river inputs play an important role in redistributing nutrients across the continental shelf (Piola et al., 2005). Moreover, most of the productivity generated on the continental shelf is transported offshore by BMC-driven cross-shelf exchanges (Berden et al., 2020). This process involves surface export of the Río de la Plata waters and the subsurface advection of Subantarctic Shelf Waters that subduct beneath the subtropical thermocline, allowing the high shelf productivity to reach the locations of our samples (Berden et al., 2020; Manta et al., 2022). These patterns are reflected in our PCA results, where samples from the northern WSA align with the PCA2, primarily driven by chlorophyll-a concentrations and iron (Fig. 5a). Instead, the southern WSA (south of 45°S) is mostly influenced by the nutrient-rich waters transported by the Malvinas Current. These cold waters flow along the continental slope extending across the shelf bottom and delivering nutrients beyond the frontal zone (Piola et al., 2010). Our results evidence that samples from the southern-WSA ordinate along the PCA1 (Fig. 5a) suggesting a macronutrient gradient controlled by nitrate, phosphate, and silicate affects their distribution. This confirms the results obtained by Paparazzo et al. (2016), who reported a south to north decreasing trend in nitrate, phosphate, and silicate concentrations along the Patagonian margin. Despite the variability the WSA exhibits, macronutrient levels generally satisfy phytoplankton requirements and do not limit primary productivity along the whole region (Brandini et al., 2000; Signorini et al., 2009). This may explain the persistent and narrow band of high chlorophyll-a concentrations observed even along the Patagonian shelf-break (Fig. 1), which closely follows the 200 m isobath and displays anomalously high peaks (Romero et al., 2006). The intense chlorophyll-a blooms are indicative of nutrient-rich upwelling and highlight the complex dynamics governing productivity in the WSA region.

Most samples from the ESA in the calibration dataset are mainly correlated with high values of chlorophyll-a and iron values (Fig. 5a), consistent with the high-productivity conditions typical of this coastal upwelling system (Barlow et al., 2009). However, a significant group of samples is observed to adjust with lower values. This inconsistency in the spatial distribution of the samples may be attributed to differences in the oceanographic features of the region. The Benguela upwelling system comprises, from north to south, areas that differ from the duration of the upwelling and level of productivity (Lutjeharms and Stockton, 1987; Ufkes et al., 2000; Petrick et al., 2015). North of of 30°S, the region is dominated by persistent upwelling and enhanced primary productivity (Andrews and Hutchings, 1980; Lutjeharms and Stockton, 1987), with upwelled cold and high-nutrient waters extending offshore in filaments (Rosell-Melé et al., 2014). Conversely, the southern area is influenced by seasonal upwelling events and generally lower nutrient availability (Andrews and Hutchings, 1980; Rosell-Melé et al., 2014; Petrick et al., 2015). These differences could be reflected in our PCA results, as the observed patterns may correspond to the regional variability within the ESA. Samples with lower PCA1 and PCA2 loading values might correspond to the southern part of the Benguela system, where productivity is comparatively reduced.

The CSA comprises the southern boundary of the South Atlantic Subtropical Gyre (Stramma and Peterson, 1990) where the persistent stratification limits the nutrient inputs to the photic zone, constraining phytoplankton growth (Eppley and Peterson, 1979; Moore et al., 2013). The spatial distribution of the samples of this region is related to lower PCA1 and PCA2 loading values. These results are consistent with the distribution patterns of

https://doi.org/10.5194/egusphere-2025-5531
Preprint. Discussion started: 28 November 2025

phytoplankton recognized in the Atlantic Ocean, which reach their lowest amount in the subtropical gyres (Cermeno et al., 2008). In our results, a group of samples, however, resulted positively correlated with nitrate and phosphate across all seasons, and winter and spring-silicate (Fig. 5a). As biogeochemical processes in oligotrophic regions have the potential to influence global elemental cycles, the higher nutrient content in the CSA could be explained due by different mechanisms such as biological fixation of N_2 gas (Michaels et al., 1996; Gruber and Sarmiento, 1997), lateral transport of dissolved organic nutrients (Rintoul and Wunsch, 1991; Williams and Follows, 1998), and mesoscale eddies-induced upwelling (McGillicuddy and Robinson, 1997; Siegel et al., 1999).

4.2 Planktonic foraminifera response to productivity-related variables in the South Atlantic

In our calibration dataset, planktonic foraminiferal assemblages reveal large compositional differences between the WSA, CSA and ESA regions. This pattern is proven by the pattern abundance of the 10 most common species (Fig. 4). Our RDA results confirm previous studies: whereas in the WSA, *G. bulloides*, *N. pachyderma* and *G. inflata* are the most abundant species (Fig. 4) (Boltovskoy et al., 1996; Chiessi et al., 2007; García Chapori and Laprida, 2021), the ESA assemblages are characterized by high abundance of *G. inflata*, *G. bulloides*, *N. incompta*, *N. dutertrei*, *O. universa* and *G. glutinata* (Giraudeau, 1993; Ufkes and Kroon, 2012, Lessa et al., 2020). The planktonic foraminifera composition of the CSA differs from those found at both South Atlantic margins, where *G. bulloides*, *N. incompta*, *G. ruber* (total), *G. falconensis* and *G. truncatulinoides* reveal a patchy pattern of high abundance (Fig. 4).

G. bulloides appears as a species mainly related to productive and nutrient-rich waters, being the only one abundant in the three regions (Fig. 6). This non-symbiotic species, typically associated with temperate to subpolar water masses, is commonly found in upwelling regions from lower latitudes (e.g., Thiede, 1975; Bé and Hutson, 1977; Kroon and Ganssen, 1988; Naidu and Malmgren, 1996; Conan and Brummer, 2000), as well as in areas of seasonally elevated primary productivity from mid- to high latitudes (e.g., Bé and Tolderlund, 1971; Schiebel and Hemleben, 2000; Mohtadi et al., 2007; Lessa et al., 2014). *N. pachyderma*, instead, reflects mainly nitrate-dominated conditions (Fig. 6a). This species, known for dominating the polar assemblages of both hemispheres (e.g., Bé and Hutson, 1977), is frequently found in upwelling regions (e.g., Conan and Brummer 2000; Darling et al., 2006; André et al., 2018). Due to its extreme habitat conditions and opportunistic strategy (cf. Ivanova et al., 1999), it has developed the ability of rapidly feeding and reproducing during the brief productive summer season (cf. Jonkers et al., 2010), feeding from phytoplankton, mainly diatoms (Spindler and Dieckmann, 1986). Its pattern distribution in our calibration dataset it is mainly associated with the nitrate-rich waters of the northward flowing Malvinas Current and Subantarctic Front. On the other hand, in our dataset *G. inflata* is negatively correlated to Nitrate_summer and Silicate_summer and slightly productive waters (Fig 6a). According to previous contributions, it has often been found to occur in the vicinity of hydrologic fronts and eddies, like the BMC region (Laprida et al., 2011) in the WSA and the ESA. This deep-dweller species, limited to mesotrophic conditions, has been interpreted to display an opportunistic behavior feeding on phytodetritus (cf. Lončarić et al., 2006; Storz et al., 2009; Chapman, 2010). *N. incompta* shows preferences for nutrient–depleted and low-productivity waters (Fig. 6a). This species is commonly associated with shallow mixed-layer depths, dominating temperate and low-productivity waters (Bé and Tolderlund, 1971; Schiebel et al., 2001), like those recorded here within the central CSA and offshore the ESA. *N. dutertrei* and *O. universa* show similar spatial distributions and abundances in the

https://doi.org/10.5194/egusphere-2025-5531
Preprint. Discussion started: 28 November 2025

calibration dataset. Interestingly, both species, with maximum abundances in the ESA (Fig. 4), have preferences for productive but nutrient-depleted waters (Fig. 6a). There, both species occur at maximum abundance north of 30°S, confirming previous contributions that linked them with the cold and enhanced primary productivity surface coastal waters (Giraudeau, 1993; Little et al., 1997). *G. ruber* and *G. falconensis* evidence to have preference for the nutrient–depleted and very low-productivity waters, and as such, they peak within the CSA (Figs. 4 and 6a). Our results confirm previous contributions that suggest that these spinose and photosynthetic symbiont-bearing species are known for being mainly associated with the mixed-layer oligotrophic waters of the Subtropical Gyre (Sierro et al., 2003; Schiebel and Hemleben, 2017; Schiebel et al., 2018; Lessa et al., 2020). *G. truncatulinoides* also shows preference for the nutrient–depleted and very low-productivity waters of the Subtropical Gyre within the CSA (Fig. 4 and Fig 6a) confirming the observations of Kucera et al. (2005). In contrast to *G. ruber* and *G. falconensis*, this is a non-spinose deep-dwelling species that usually reflects the conditions of the permanent thermocline, where photosynthetic activity is constrained by the low light availability (Schiebel and Hemleben, 2017). Finally, *G. glutinata* prefers environments with slightly low chlorophyll-a and nutrient concentrations associated with the southern limb of the Subtropical Gyre. Its position, together with *T. iota*, *G. humilis*, and *G. nitida* (Fig 6a) aligns with the observations of Lessa et al. (2020), who reported these species as co-occurring within the surface faunas of the Gyre and Agulhas Leakage regions.

4.3 Transfer function selection

The application of transfer functions assumes that the assemblages' structure of the analyzed group responds to environmental forcings, and that the principal driving factors are known (Birks, 1995). This assumption presents significant challenges, as it required both prior ecological knowledge and objective procedures for selecting relevant variables. Regardless of the approach, decision makers must integrate ecological information such as output from ecological models with environmental considerations such as spatial variability or chaotic processes. In a paleoceanographic context, variable selection is often difficult by the high degree of collinearity among candidate oceanographic factors. Previous transfer function studies had aimed to present any model with a decent predictive performance and, if the calibration dataset was spatially autocorrelated or the reconstructed variable was not significant, they recommended caution when the results were interpreted or even considered the model or variable to be useless (e.g., Amesbury et al., 2013; Hernandez-Almeida et al., 2020; Chen et al., 2020; Hohmann et al., 2023). Here we suggest a different perspective, mostly focusing on the purpose of the model (or study): whether it is to be used purely to gain understanding, purely for prediction, or both. The reconstructed variable can be safely interpreted if we are environmentally aware using the different statistical models.

Our results confirm that planktonic foraminiferal assemblages respond to other environmental gradients besides temperature (Lessa et al., 2020; García Chapori and Laprida, 2021), and suggest that it is possible to extract information from the same fossil planktonic foraminifera assemblage on past variability for different environmental drivers. However, the presence of several interacting biotic and abiotic processes influencing planktonic foraminifera distribution could manifest complex species–environment relationships. These responses surely exist in the ocean and we often cannot detect them because their signal is weak or they are confused with sampling noise, bias or spatial autocorrelation. As a result, the detected signature of the environmental variables that exhibit spatial dependence in the calibration dataset is likely the result of integrating all information sources

https://doi.org/10.5194/egusphere-2025-5531
Preprint. Discussion started: 28 November 2025

from regions with different environmental drivers, rather than a single, uniform response. A stronger characterization of each gradient would require a local constrained analysis which inevitably leads to a compromise in the analogues of the resulting ecological models and restricts their applicability to past oceanographic scenarios. Moreover, intrinsic biological features such as cryptic diversity, life-cycle dynamics, or seasonal species blooms may further constrain the ability of transfer functions to capture broad aspects of the species-environment relationship. These factors, in theory, should impact the different transfer function methods based on various foundational principles differently (Kucera et al., 2005).

Since WA method averages the ecological tolerances (Birks et al., 1990), it appears less sensitive than other methods to the overestimation caused by the spatial autocorrelation. In this context, after evaluating a wide range of statistical approaches, we chose the WATOL_inv model to perform the downcore reconstruction since it effectively reveals and describes the species-environment relationship. The use of h-block cross-validation approach effectively mitigated the influence of spatial autocorrelation and facilitated the identification of the optimal h-value for obtaining unbiased performance estimates. By partitioning the dataset into spatially independent blocks and accounting for the dependence structure, this method reduced the risk of overfitting (Trachsel and Telford, 2016). By selecting WATOL_inv as the final model, we adopted an approach well suited to situations where species show a clear unimodal response to a dominant gradient, in this case, surface Nitrate_summer. The combined strategy of accounting for autocorrelation through h-block cross validation and identifying the most spatially stable and ecologically meaningful variable allowed us to select a model that best captures the underlying species–environment relationship while ensuring more robust paleoceanographic reconstructions.

4.4 Holocene paleoproductivity reconstruction in the BMC (WSA)

Surface Nitrate_summer estimates obtained for core GeoB2806-4 revealed that paleoproductivity in the BMC influence zone has been subject to notable changes along the Holocene. Our reconstruction reveals a marked decrease in Nitrate_summer concentration between ~11.7 – 5 cal kyrs BP (Fig. 9a). This trend coincides with a progressive increase in the annual mixed-layer temperature of ~3ºC (Fig. 9b). As the annual mixed-layer temperature increased, stratified conditions of the water column also increased, provoking a progressive depletion of nitrate from the upper layers since phytoplankton communities consume a large amount of nutrients under stratified conditions (Signorini et al., 2009). As nitrate availability declined, the system reflected a scenario of nearly complete nutrient utilization, which is usually associated with enhanced primary productivity (Sverdrup, 1953; Paparazzo et al, 2010). Thus, a progressive biological uptake during the early-mid Holocene within the BMC influence zone can be interpreted. Between ~5 - 2 cal kyrs BP, instead, the increase in surface nitrate levels and decrease in mixed-layer temperatures (Fig. 9a-b) would reflect the opposite pattern, where the lower nutrient utilization would suggest lower biological uptake. Nowadays, the cold subantarctic waters carried by the Malvinas Current are the main source of nitrate content to the WSA, particularly the Argentine continental margin (Carreto et al., 1995). The Malvinas Current flows northward along the margin until it encounters the Brazil Current ~38S°. There, at the BMC, primary productivity varies mostly influenced by changes in the dynamics of both currents, specially the seasonal shifts of the BMC (García et al., 2004; Saraceno et al., 2005; Artana et al., 2019) that occur in response to changes in the intensity/position of the northern portion of the westerlies (Lumpkin and Garzoli, 2011). Additionally, other factors can also enhance the nutrients carried by the Malvinas Current, such as the

https://doi.org/10.5194/egusphere-2025-5531
Preprint. Discussion started: 28 November 2025

strengthening of the Patagonian shelf-break upwelling (García et al., 2008), and the intensification of the wind that carries continental dust to the ocean (Moore et al., 2001). These high levels of surface nitrate support the high phytoplankton biomass associated with the shelf-break front throughout summer and autumn (Carreto et al., 1995). During the late Quaternary, shifts of the BMC would have been wider than today (see García Chapori et al., 2022 references therein). According to Voigt et al. (2015), between ~11.7 and 5.5 cal kyr BP, the position of the BMC experienced a gradual southward displacement of 1º (Fig. 9c) in response to the poleward migration of the westerlies until it reached its current position. An equatorward position of the BMC during the onset of the Holocene would have led to major advection of the Malvinas Current, intensifying the shelf-break upwelling of Patagonia, and thereby increasing the nitrate supply and cooling the mixed-layer waters at the core site. The intervening colder nutrient-rich subantarctic waters provided the necessary nutrients for biomass growth. Towards the mid-Holocene, the southward displacement of the BMC (Voigt et al., 2015) provoked a temperature increase leading to a decrease of surface nitrate content due to enhanced productivity. Records from the Brazilian slope revealed warmer conditions during early to mid-Holocene transition (Pivel et al., 2013; Chiessi et al., 2014; Pereira et al., 2018), attributed to a more vigorous Brazil Current transport, confirming the southward shift of the BMC. Within the BMC, however, other local factors affect the primary productivity nowadays, in particular the Plata Plume Water (Carreto et al., 1986), which provides ca. 8×10^7 t yr^{-1} of suspended sediment load to the WSA (Depetris et al., 2003), representing an important source of nutrient input. During the mid-Holocene, drier conditions over southeastern South America, related to a weakening of the southeastward low-level jet moisture transport (Wang et al., 2007), would have reduced rainfall over the Río de la Plata drainage basin leading to a low terrigenous input (de Mahiques et al., 2009). These conditions persisted until the mid- to late Holocene transition. These processes could have implied a decrease in the Plata Plume Water nutrient input, leaving the nutrient supply from the Malvinas Current as the main source sustaining the biological productivity at the BMC. During the early Late Holocene (~4 – 2 cal kyr BP), when the surface Nitrate_summer reached its highest levels (Fig. 9a), the slight cooling (ca. 0.6ºC) and the northward displacement of the BMC (Fig. 9b-c) suggest a major influence of the Malvinas Current at the core site. These results confirm the dinoflagellate records from the southern Brazil margin that also evidence a northward displacement of the BMC between ~4 - 2 cal kyr BP (Gu et al., 2018), and are in accordance with paleolimnological records from the Patagonia steppe (Douglass et al., 2005; Siani et al., 2010) and model simulations (Varma et al., 2012; Berman et al., 2016) that suggest an equatorward shift of the westerlies during the late Holocene. However, the higher nitrate concentrations relative to those of the early Holocene would imply more stratified conditions at the core site during the early Late Holocene.

https://doi.org/10.5194/egusphere-2025-5531
Preprint. Discussion started: 28 November 2025

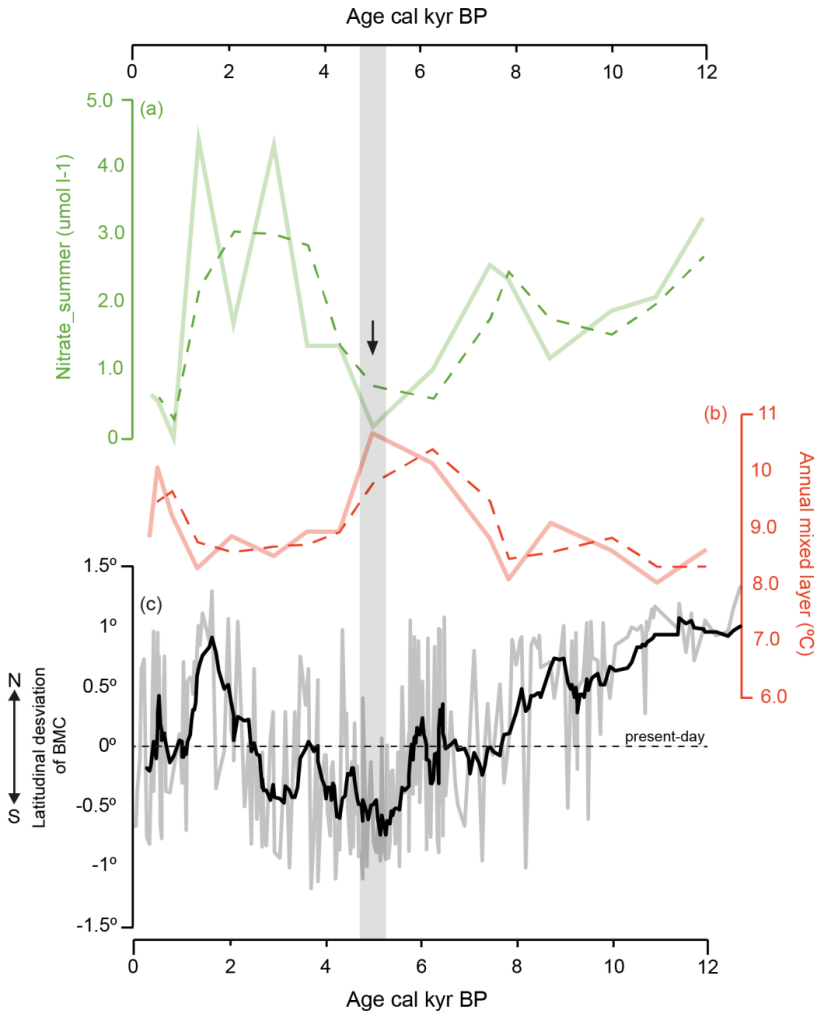

Figure 9: (a) Nitrate_summer reconstructions for the GeoB2806-4 core derived from the WATOL_inv model (dash green line, moving average); (b) Annual mixed-layer temperature modified from Garcia Chapori and Laprida (2022) (dash red line, moving average); (c) Latitudinal deviation of the Brazil-Malvinas Confluence (BMC) from its present-day position, estimated from the $\delta^{18}O_{ivc}$ GeoB13862-1 record (in degrees of latitude), using data from Voigt et al. (2015).

5. Conclusions

In this study we analyze the relationship between planktonic foraminifera distribution present in modern sediment samples and a suite of potential driving productivity-related variables in a calibration dataset that comprises the South Atlantic. Our results indicate that productivity-related variables are relevant drivers of the modern planktonic foraminiferal assemblage structure. The identification of surface summer nitrate concentration as the principal driver represents a novel outcome, suggesting that planktonic foraminifera exhibit a more complex ecological response to the environmental variables than usually expected. Additionally, nutrient-related gradients

https://doi.org/10.5194/egusphere-2025-5531
Preprint. Discussion started: 28 November 2025

emerge as independent drivers that account for significant aspects of the spatial distribution of planktonic foraminifera. The calibration dataset compiled includes key oceanographic features allowing us to distinguish three different regions: the western South Atlantic, central South Atlantic, and eastern South Atlantic. The chosen regression model for reconstructing surface summer nitrate is WATOL_inv with h-block cross validation (r^2_{cv} = 0.938; RMSEP = 1.578 umol l^{-1}). The reconstructed variations inferred from sediment core GeoB2806-4 suggest that, during the Holocene, surface summer nitrate was linked to the latitudinal displacement of the Brazil-Malvinas Confluence, ultimately driven by shifts of the northern portion of the South Westerly Winds. Equatorward shifts of the winds belt enhanced the advection of the Malvinas Current, increasing the nitrate supply and cooling the mixed layer at the core site, while poleward displacements allowed the stratification of the mixed layer intensifying the biological uptake, and therefore reduced the nitrate availability.

This study demonstrates that, when applied with ecological awareness and appropriate statistical tools, reconstructions of different environmental variables can yield meaningful results. Therefore, under certain conditions and with careful attention to the proxy ecology, variables selection, and model sensitivity, reliable reconstructions are feasible. However, determining whether such reconstructions can be generalized across broader micropaleontological datasets remains an open question.

6. Data availability

The core-top samples data reported in this paper are archived in PANGAEA (https://doi.org/10.1594/PANGAEA.949250). Sediment core GeoB2406-4 data was extracted from PANGAEA (https://doi.org/10.1594/PANGAEA.845640).

7. Author contribution

Paula B. Albarracin: Writing – original draft, Methodology, Validation, Visualization, Data curation, Investigation, Formal analysis, Conceptualization. **Natalia García Chapori**: Writing – review and editing, conceptualization, Formal analysis, Visualization, Supervision. **Cecilia Laprida**: Writing – review and editing, conceptualization, Visualization, Formal analysis, project administration, funding acquisition.

8. Competing interests

The authors declare that they have no conflict of interest.

9. Acknowledgements.

This research was supported by the Argentine National Scientific and Technical Research Council (CONICET; project PIP 11220220100103CO) and the University of Buenos Aires (project UBACyT 20020190100204BA).

10. References

Amesbury, M. J., Mallon, G., Charman, D. J., Hughes, P. D. M., Booth, R. K., Daley, T. J., and Garneau, M.: Statistical testing of a new testate amoeba-based transfer function for water-table depth reconstruction on

https://doi.org/10.5194/egusphere-2025-5531
Preprint. Discussion started: 28 November 2025

ombrotrophic peatlands in north-eastern Canada and Maine, United States, J. Quaternary Sci., 28, 27–39, https://doi.org/10.1002/jqs.25842, 2013.

André, A., Quillévéré, F., Schiebel, R., Morard, R., Howa, H., Meilland, J., and Douady, C.: Disconnection between genetic and morphological diversity in the planktonic foraminifer Neogloboquadrina pachyderma from the Indian Sector of the Southern Ocean, Mar. Micropaleontol., 144, 14–24, https://doi.org/10.1016/j.marmicro.2018.08.001, 2018.

Andrews, W. R. H. and Hutchings, L.: Upwelling in the southern Benguela Current, Prog. Oceanogr., 9, 1–81, https://doi.org/10.1016/0079-6611(80)90015-4, 1980.

Artana, C., Provost, C., Lellouche, J.M., Rio, M.H., Ferrari, R., and Sennéchael, N.: The Malvinas Current at the Confluence with the Brazil Current: Inferences from 25 years of Mercator Ocean reanalysis, J. Geophys. Res.-Oceans, 124, 7178–7200, https://doi.org/10.1029/2019JC015289, 2019.

Barlow, R., Lamont, T., Mitchell-Innes, B., Lucas, M., and Thomalla, S.: Primary production in the Benguela ecosystem, 1999–2002, Afr. J. Mar. Sci., 31, 97–101, https://doi.org/10.2989/AJMS.2009.31.1.10.780, 2009.

Barré, N., Provost, C., and Saraceno, M.: Spatial and temporal scales of the Brazil–Malvinas Current confluence documented by simultaneous MODIS Aqua 1.1-km resolution SST and color images, Adv. Space Res., 37, 770–786, https://doi.org/10.1016/j.asr.2005.07.031, 2006.

Bé, A. W. H.: An ecological, zoogeographic, and taxonomic review of recent planktonic foraminifera, in: Oceanic Micropaleontology, Vol. 1, edited by: Ramsay, A. T. S., Elsevier, New York, 1–100, 1977.

Bé, A. W. H. and Hutson, W. H.: Ecology of Planktonic Foraminifera and Biogeographic Patterns of Life and Fossil Assemblages in the Indian Ocean, Micropaleontology, 23, 369–414, https://doi.org/10.2307/1485406, 1977.

Bé, A. W. H. and Tolderlund, D. S.: Distribution and ecology of planktonic foraminifera in surface waters of the Atlantic and Indian Oceans, in: The Micropaleontology of Oceans, edited by: Funnell, B. and Riedel, W., Cambridge Univ. Press, London, 105–150, 1971.

Berden, G., Charo, M., Möller, O. O. Jr., and Piola, A. R.: Circulation and hydrography in the western South Atlantic shelf and export to the deep adjacent ocean: 30°S to 40°S, J. Geophys. Res.-Oceans, 125, e2020JC016500, https://doi.org/10.1029/2020JC016500, 2020.

Berger, W. H.: Sedimentation of planktonic foraminifera, Mar. Geol., 11, 325–358, 1971.

Berman, A. L., Silvestri, G. E., Rojas, M., and Tonello, M. T.: Accelerated greenhouse gases versus slow insolation forcing induced climate changes in southern South America since the Mid-Holocene, Clim. Dynam., https://doi.org/10.1007/s00382-016-3081-z , 2016.

Bijma, J., Faber, W. W., and Hemleben, C.: Temperature and salinity limits for growth and survival of some planktonic foraminifers in laboratory cultures, J. Foraminifer. Res., 20, 95–116, https://doi.org/10.2113/gsjfr.20.2.95, 1990.

https://doi.org/10.5194/egusphere-2025-5531
Preprint. Discussion started: 28 November 2025

Birks, H. J. B.: Quantitative palaeoenvironmental reconstructions, in: Statistical Modelling of Quaternary Science Data (Technical Guide 5), edited by: Maddy, D. and Brew, J. S., Quaternary Research Association, Cambridge, 161–254, 1995.

Birks, H. J. B.: Numerical tools in palaeolimnology: progress, potentialities and problems, J. Paleolimnol., 20, 307–332, 1998.

Birks, H. J. B., Line, J. M., Juggins, S., Stevenson, A. C., and ter Braak, C. J. F.: Diatoms and pH reconstruction, Philos. Trans. R. Soc. B, 327, 263–278, 1990.

Birks, H. J. B., Heiri, O., Seppä, H., and Bjune, A. E.: Strengths and weaknesses of quantitative climate reconstructions based on Late-Quaternary biological proxies, Open Ecol. J., 3, 68–110, 2010.

Boltovskoy, E. and Wright, R.: Recent Foraminifera, Junk, The Hague, 515 pp., 1976.

Boltovskoy, E., Boltovskoy, D., Correa, N., and Brandini, F.: Planktic foraminifera from the Southwestern Atlantic (30°–60°S): species-specific patterns in the upper 50 m, Mar. Micropaleontol., 28, 53–72, https://doi.org/10.1016/0377-8398 (95)00045-3, 1996.

Brandhorst, W. and Castello, J. P.: Evaluación de los recursos de anchoita (Engraulis anchoita) frente a la Argentina y Uruguay. I. Las condiciones oceanográficas, sinopsis del conocimiento actual sobre la anchoita y el plan para su evaluación, Proyecto Desarrollo Pesquero, FAO, Publicación n° 29, 63 pp., 1971.

Brandini, F., Boltovskoy, D., Piola, A., Kocmur, S., Rottgers, R., Abreu, P., and Mendes, D.: Multiannual trends in fronts and distribution of nutrients and chlorophyll in the southwestern Atlantic, Deep-Sea Res. Pt. I, 47, 1015–1033, https://doi.org/10.1016/S0967-0637 (99)00074-X, 2000.

Burman, P., Bhow, E., and Nonal, D.: A cross-validatory method for dependent data, Biometrika, 81, 351–358, https://doi.org/10.1093/biomet/81.2.351, 1994.

Carreto, J. I., Negri, R. M., and Benavides, H. R.: Algunas características del florecimiento del fitoplancton en el Frente del Río de la Plata. Parte 1: Los sistemas nutritivos, Rev. Invest. Des. Pesq., 5, 7–29, 1986.

Carreto, J. I., Lutz, V. A., Carignan, M. O., Cucchi Colleoni, A. D., and de Marco, S. G.: Hydrography and chlorophyll a in a transect from the coast to the shelf-break in the Argentinian Sea, Cont. Shelf Res., 15, 315–336, 1995.

Cermeno, P., Dutkiewicz, S., Harris, R. P., Follows, M., Schofield, O., and Falkowski, P. G.: The role of nutricline depth in regulating the ocean carbon cycle, Proc. Natl. Acad. Sci. USA, 105, 20344–20349, https://doi.org/10.1073/pnas.0811302106 , 2008.

Chapman, M. R.: Seasonal production patterns of planktonic Foraminifera in the NE Atlantic Ocean: implications for paleotemperature and hydrographic reconstructions, Paleoceanography, 25, PA2203, https://doi.org/10.1029/2008PA001708, 2010.

Chen, F., Zhang, J., Liu, J., Cao, X., Hou, J., Zhu, L., Xu, X., Liu, X., Wang, M., Wu, D., Huang, L., Zeng, T., Zhang, S., Huang, W., Zhang, X., and Yang, K.: Climate change, vegetation history, and landscape responses

https://doi.org/10.5194/egusphere-2025-5531
Preprint. Discussion started: 28 November 2025

on the Tibetan Plateau during the Holocene: a comprehensive review, Quat. Sci. Rev., 243, 1–21, https://doi.org/10.1016/j.quascirev.2020.106444, 2020.

Chiessi, C. M., Ulrich, S., Mulitza, S., Pätzold, J., and Wefer, G.: Signature of the Brazil–Malvinas Confluence (Argentine Basin) in the isotopic composition of planktonic foraminifera from surface sediments, Mar. Micropaleontol., 64, 52–66, https://doi.org/10.1016/j.marmicro.2007.02.002, 2007.

Chiessi, C. M., Mulitza, S., Groeneveld, J., Silva, J. B., Campos, M. C., and Gurgel, M. H. C.: Variability of the Brazil Current during the late Holocene, Palaeogeogr. Palaeoclimatol. Palaeoecol., 415, 28–36, https://doi.org/10.1016/j.palaeo.2013.12.005 , 2014.

Conan, S. M.H. and Brummer, G.-J. A.: Fluxes of planktic foraminifera in response to monsoonal upwelling on the Somalia Basin margin, Deep-Sea Res. Pt. II, 47, 2207–2227, https://doi.org/10.1016/S0967-0645 (00)00019-0, 2000.

Darling, K. F., Kucera, M., Kroon, D., and Wade, C. M.: A resolution for the coiling direction paradox in Neogloboquadrina pachyderma, Paleoceanography, 21, PA2011, https://doi.org/10.1029/2005PA001189, 2006.

Dave, A. C., Barton, A. D., Lozier, M. S., and McKinley, G. A.: What drives seasonal change in oligotrophic area in the subtropical North Atlantic?, J. Geophys. Res.-Oceans, 120, 3958–3969, https://doi.org/10.1002/2015JC010787, 2015.

de Mahiques, M. M., Wainer, I. K. C., Burone, L., Nagai, R., de Mello e Sousa, S. H., Figueira, R. C. L., da Silveira, I. C. A., Bícego, M. C., Vicente Alves, D. P., and Hammer, Ø.: A high-resolution Holocene record on the Southern Brazilian shelf: paleoenvironmental implications, Quat. Int., 206, 52–61, https://doi.org/10.1016/j.quaint.2008.10.008 , 2009.

de Vernal, A., Eynaud, F., Henry, M., Hillaire-Marcel, C., Londeix, L., Mangin, S., Matthiessen, J., Marret, F., Radi, T., Rochon, A., Solignac, S., and Turon, J. L.: Reconstruction of sea-surface conditions at middle to high latitudes of the Northern Hemisphere during the Last Glacial Maximum (LGM) based on dinoflagellate cyst assemblages, Quat. Sci. Rev., 24, 897–924, https://doi.org/10.1016/j.quascirev.2004.06.014, 2005.

Depetris, P. J. and Paolini, J. E.: Biogeochemical aspects of South American rivers: The Paraná and the Orinoco, in: Biogeochemistry of Major World Rivers, Scope 42, edited by: Degens, E. T., Kempe, S., and Richey, J. R., John Wiley and Sons, Chichester, 105–125, 1991.

Depetris, P. J., Probst, J.L., Pasquini, A. I., and Gaiero, D. M.: The geochemical characteristics of the Paraná suspended sediment load: an initial assessment, Hydrol. Process., 17, 1267–1277, 2003.

Dong, S., Goni, G., Domingues, R., Bringas, F., Goes, M., Christophersen, J., and Baringer, M.: Synergy of in situ and satellite ocean observations in determining meridional heat transport in the Atlantic Ocean, J. Geophys. Res.-Oceans, 126, e2020JC017073, https://doi.org/10.1029/2020JC017073, 2021.

https://doi.org/10.5194/egusphere-2025-5531
Preprint. Discussion started: 28 November 2025

Douglass, D. C., Singer, B. S., Kaplan, M. R., Ackert, R. P., Mickelson, D. M., and Caffee, M. W.: Evidence of early Holocene glacial advances in southern South America from cosmogenic surface exposure dating, Geology, 33, 237–240, https://doi.org/10.1130/G21144.1 , 2005.

Eppley, R. W. and Peterson, B. J.: Particulate organic matter flux and planktonic new production in the deep ocean, Nature, 282, 677–680, https://doi.org/10.1038/282677a0, 1979.

Fatela, F. and Taborda, R.: Confidence limits of species proportions in microfossil assemblages, Mar. Micropaleontol., 45, 169–174, https://doi.org/10.1016/S0377-8398(02)00021-X, 2002.

Field, C. B., Behrenfeld, M. J., Randerson, J. T., and Falkowski, P. G.: Primary production of the biosphere: integrating terrestrial and oceanic components, Science, 281, 237–240, https://doi.org/10.1126/science.281.5374.237, 1998.

Forster, P. M., Smith, C. J., Walsh, T., Lamb, W. F., Lamboll, R., Hauser, M., Ribes, A., Rosen, D., Gillett, N., Palmer, M. D., Rogelj, J., von Schuckmann, K., Seneviratne, S. I., Trewin, B., Zhang, X., Allen, M., Andrew, R., Birt, A., Borger, A., Boyer, T., Broersma, J. A., Cheng, L., Dentener, F., Friedlingstein, P., Gutiérrez, J. M., Gütschow, J., Hall, B., Ishii, M., Jenkins, S., Lan, X., Lee, J.-Y., Morice, C., Kadow, C., Kennedy, J., Killick, R., Minx, J. C., Naik, V., Peters, G. P., Pirani, A., Pongratz, J., Schleussner, C.-F., Szopa, S., Thorne, P., Rohde, R., Rojas Corradi, M., Schumacher, D., Vose, R., Zickfeld, K., Masson-Delmotte, V., and Zhai, P.: Indicators of Global Climate Change 2022: annual update of large-scale indicators of the state of the climate system and human influence, Earth Syst. Sci. Data, 15, 2295–2327, https://doi.org/10.5194/essd-15-2295-2023, 2023.

Gallego, D., García-Herrera, R., Tomety, F. S., et al.: Historical record of upwelling-favorable winds in Southern Benguela 1833–2014, npj Clim. Atmos. Sci., 8, 36, https://doi.org/10.1038/s41612-025-00925-0, 2025.

García, C. A. E., Sarma, Y. V. B., Mata, M. M., and García, V. M. T.: Chlorophyll variability and eddies in the Brazil–Malvinas Confluence region, Deep-Sea Res. Pt. II, 51, 159–172, https://doi.org/10.1016/j.dsr2.2003.07.016, 2004.

García, H. E., Locarnini, R. A., Boyer, T. P., Antonov, J. I., Baranova, O. K., Zweng, M. M., Reagan, J. R., and Johnson, D. R.: World Ocean Atlas 2013. Vol. 4: Dissolved Inorganic Nutrients (phosphate, nitrate, silicate), NOAA Atlas NESDIS 76, 25 pp., 2013.

García, V. M. T., García, C. A. E., Mata, M. M., Pollery, R. C., Piola, A. R., Signorini, S. R., McClain, C. R., and Iglesias-Rodriguez, M. D.: Environmental factors controlling the phytoplankton blooms at the Patagonia shelf-break in spring, Deep-Sea Res., 55, 1150–1166, https://doi.org/10.1016/j.dsr.2008.04.011 , 2008.

García Chapori, N. and Kucera, M.: Planktonic foraminifera census counts from the western South Atlantic, PANGAEA, https://doi.org/10.1594/PANGAEA.907931, 2019.

García Chapori, N. and Laprida, C.: Planktonic foraminifera assemblages from the Brazil–Malvinas Confluence: palaeoceanographic implications of sub-surface temperature reconstructions in the western South Atlantic, Lethaia, 54, 477–494, https://doi.org/10.1111/let.12416, 2021.

García Chapori, N., Chiessi, C. M., Bickert, T., and Laprida, C.: Sea-surface temperature reconstruction of the western South Atlantic: new planktonic foraminiferal correlation function, Palaeogeogr. Palaeoclimatol. Palaeoecol., 425, 67–75, https://doi.org/10.1016/j.palaeo.2015.02.027, 2015.

García Chapori, N., Laprida, C., Lo Prete, D., Chiessi, C. M., Mayr, C., and Violante, R. A.: Holocene palaeoceanographic history of the western South Atlantic, J. S. Am. Earth Sci., 117, 103896, https://doi.org/10.1016/j.jsames.2022.103896 , 2022.

Garzoli, S. L. and Matano, R.: The South Atlantic and the Atlantic Meridional Overturning Circulation, Deep-Sea Res. Pt. II, 58, 1837–1847, https://doi.org/10.1016/j.dsr2.2010.10.063, 2011.

Giraudeau, J.: Planktonic foraminiferal assemblages in surface sediments from the southwest African continental margin, Mar. Geol., 110, 47–62, https://doi.org/10.1016/0025-3227 (93)90104-4, 1993.

Gordon, A. L. and Greengrove, C. L.: Geostrophic circulation of the Brazil–Falkland Confluence, Deep-Sea Res. Pt. A, 33, 573–585, https://doi.org/10.1016/0198-0149(86)90054-3, 1986.

Gregg, W. W., Ginoux, P., Schopf, P. S., and Casey, N. W.: Phytoplankton and iron: validation of a global three-dimensional ocean biogeochemical model, Deep-Sea Res. Pt. II, 50, 3143–3169, https://doi.org/10.1016/j.dsr2.2003.07.013, 2003.

Gruber, N. and Sarmiento, J. L.: Global patterns of marine nitrogen fixation and denitrification, Global Biogeochem. Cy, 11, 235–266, https://doi.org/10.1029/97GB00077, 1997.

Gu, F., Chiessi, C. M., Zonneveld, K. A. F., and Behling, H.: Late Quaternary environmental dynamics inferred from marine sediment core GeoB6211-2 off southern Brazil, Palaeogeogr. Palaeoclimatol. Palaeoecol., 496, 48–61, https://doi.org/10.1016/j.palaeo.2018.01.016 , 2018.

Hemleben, C., Spindler, M., and Anderson, O. R.: Modern Planktonic Foraminifera, Springer, Berlin, 363 pp., 1989.

Hernández-Almeida, I., Boltovskoy, D., Kruglikova, S. B., and Cortese, G.: A new radiolarian transfer function for the Pacific Ocean and application to fossil records: Assessing potential and limitations for the last glacial–interglacial cycle, Global Planet. Change, 190, 103186, https://doi.org/10.1016/j.gloplacha.2020.103186, 2020.

Hohmann, S., Kucera, M., and de Vernal, A.: Disentangling environmental drivers of subarctic dinocyst assemblage compositional change during the Holocene, Clim. Past, 19, 2027–2051, https://doi.org/10.5194/cp-19-2027-2023, 2023.

Hutson, W. H. and Prell, W. L.: A paleoecological transfer function, FI-2, for Indian Ocean planktonic foraminifera, J. Paleontol., 54, 381–399, 1980.

Imbrie, J. and Kipp, N. G.: A new micropaleontological method for quantitative paleoclimatology: application to a late Pleistocene Caribbean core, in: The Late Cenozoic Glacial Ages, edited by: Turekian, K. K., Yale University Press, New Haven, 71–181, https://doi.org/10.1016/0033-5894(73)90051-3, 1971.

Ivanova, E. M., Conan, S. M.-H., Peeters, F. J. C., and Troelstra, S. R.: Living Neogloboquadrina pachyderma sin and its distribution in the sediments from Oman and Somalia upwelling areas, Mar. Micropaleontol., 36, 91–107, https://doi.org/10.1016/S0377-8398(98)00027-9, 1999.

Jackson, D. A.: Stopping rules in principal components analysis: a comparison of heuristical and statistical approaches, Ecology, 74, 2204–2214, https://doi.org/10.2307/1939574, 1993.

Jonkers, L. and Kucera, M.: Global analysis of seasonality in the shell flux of extant planktonic foraminifera, Biogeosciences, 12, 2207–2226, https://doi.org/10.5194/bg-12-2207-2015, 2015.

Jonkers, L., Brummer, G.-J. A., Peeters, F. J. C., van Aken, H. M., and De Jong, M. F.: Seasonal stratification, shell flux, and oxygen isotope dynamics of left-coiling N. pachyderma and T. quinqueloba in the western subpolar North Atlantic, Paleoceanography, 25, PA2204, https://doi.org/10.1029/2009PA001849, 2010.

Jonkers, L., Strack, T., Alonso-García, M., D'haenens, S., Huber, R., Kucera, M., Hernández-Almeida, I., Jones, C. L. C., Metcalfe, B., Saraswat, R., Silye, L., Verma, S. K., Abd Malek, M. N., Auer, G., Barbosa, C. F., Bárcena, M. A., Baumann, K.-H., Boscolo-Galazzo, F., Calvelo, J. A. S., Capotondi, L., Cardich, J., Carvajal-Chitty, H., Chroustová, M., Coxall, H. K., de Mello, R. M., de Vernal, A., Diz, P., Edgar, K. M., Filipsson, H. L., Fraguas, Á., Furlong, H. L., Galli, G., García Chapori, N. L., Granger, R., Groeneveld, J., Imam, A., Jackson, R., Lazarus, D., Meilland, J., Molčan Matejová, M., Morard, R., Morigi, C., Nielsen, S. N., Ochoa, D., Petrizzo, M. R., Rigual-Hernández, A. S., Rillo, M. C., Staitis, M. L., Tanık, G., Tapia, R., Vats, N., Wade, B. S., and Weinmann, A. E.: Community guidelines to increase the reusability of marine microfossil assemblage data, J. Micropalaeontol., 44, 145–168, https://doi.org/10.5194/jm-44-145-2025, 2025.

Juggins, S.: C2 version 1.5 user guide: software for ecological and palaeoecological data analysis and visualisation, Newcastle University, Newcastle upon Tyne, UK, 73 pp., 2007.

Juggins, S.: Quantitative reconstructions in palaeolimnology: new paradigm or sick science?, Quat. Sci. Rev., 64, 20–32, https://doi.org/10.1016/j.quascirev.2012.12.014, 2013.

Juggins, S.: Rioja: Analysis of Quaternary science data, R package, available at: https://cran.r-project.org/web/packages/rioja/, 2017.

Juggins, S. and Birks, H. J. B.: Quantitative environmental reconstructions from biological data, in: Tracking environmental change, edited by: Birks, H. J. B., Lotter, A. F., Juggins, S., and Smol, J. P., Springer, Dordrecht, 431–494, https://doi.org/10.1007/978-94-007-2745-8_14, 2012.

Jullion, L., Heywood, K. J., Naveira Garabato, A. C., and Stevens, D. P.: Circulation and water mass modification in the Brazil–Malvinas Confluence, J. Phys. Oceanogr., 40, 845–864, https://doi.org/10.1175/2009JPO4174.1, 2010.

Kasten, S., Schwenk, T., Aromokeye, D. A., Baques, M., Baumann, K. H., Bergenthal, M., Bösche, J., Bozzano, G., Brune, R., Bülten, J., Chiessi, C. M., Coffinet, S., Crivellari, S., Dehning, K., Dohrmann, I., Dröllner, M., Düßmann, R., Durica, J. T., Frederichs, T., Garcia Chapori, N., Gonzales, L. N., Hanebuth, T. J. J., Hilgenfeldt, C., Hüttich, D., Jones, C. K., Klann, M., Klar, S., Klein, T., Kockisch, B., Köster, M., Lantzsch, H., Linowski, E., Long, J. H., Melcher, A. C., Ogunleye, O. J., Pereyra, N., Rehage, R., Riedinger, N., Rosiak, U., Schmidt,

W., Schnakenberg, A., Spieß, V., Steinmann, L., Thieblemont, A., Volz, J., Warnke, F., Warratz, G., Wenau, S., and Zonneveld, K. A.: Dynamics of sedimentation processes and their impact on biogeochemical reactions on the continental slope off Argentina and Uruguay (MARUM), Cruise No. SO260/Leg 1 & Leg 2, Leg 1: 12–30 January 2018, Buenos Aires (Argentina)–Montevideo (Uruguay); Leg 2: 2–14 February 2018, Montevideo (Uruguay)–Buenos Aires (Argentina), DosProBio, https://doi.org/10.2312/cr_so260, 2019.

Kersalé, M., Meinen, C. S., Perez, R. C., Piola, A. R., Speich, S., Campos, E. J. D., et al.: Multi-year estimates of daily heat transport by the Atlantic meridional overturning circulation at 34.5°S, J. Geophys. Res.-Oceans, 126, e2020JC016947, https://doi.org/10.1029/2020JC016947, 2021.

Kroon, D. and Ganssen, G.: Northern Indian Ocean upwelling cells and the stable isotope composition of living planktic foraminifers, in: Planktonic Foraminifers as Tracers of Ocean-Climate History, edited by: Brummer, G.J. A. and Kroon, D., Free Univ. Press, Amsterdam, 299–317, https://doi.org/10.1016/0198-0149(89)90102-7, 1988.

Kucera, M.: Planktonic Foraminifera as tracers of past oceanic environments, in: Proxies in Late Cenozoic Paleoceanography, Developments in Marine Geology, vol. 1, edited by: Hillaire-Marcel, C. and de Vernal, A., 213–262, Elsevier, Amsterdam, https://doi.org/10.1016/S1572-5480(07)01011-1, 2007.

Kucera, M., Weinelt, M., Kiefer, T., Pflaumann, U., Hayes, A., Chen, M.-T., Mix, A. C., Barrows, T. T., Cortijo, E., Duprat, J., Juggins, S., and Waelbroeck, C.: Reconstruction of sea-surface temperatures from assemblages of planktonic foraminifera: multi-technique approach based on geographically constrained calibration data sets and its application to glacial Atlantic and Pacific Oceans, Quat. Sci. Rev., 24, 951–998, https://doi.org/10.1016/j.quascirev.2004.07.014, 2005.

Laprida, C., García Chapori, N., Chiessi, C. M., Violante, R. A., Watanabe, S., and Totah, V.: Middle Pleistocene sea surface temperature in the Brazil–Malvinas Confluence Zone: Paleoceanographic implications based on planktonic foraminifera, Micropaleontology, 57, 183–194, doi:10.47894/mpal.57.2.06, 2011.

Lee, T., Rand, D., Lisiecki, L. E., Gebbie, G., and Lawrence, C.: Bayesian age models and stacks: combining age inferences from radiocarbon and benthic δ18O stratigraphic alignment, Clim. Past, 19, 1993–2012, https://doi.org/10.5194/cp-19-1993-2023, 2023.

Lepš, J. and Šmilauer, P.: Multivariate Analysis of Ecological Data using CANOCO, Cambridge University Press, Cambridge, 2003.

Lessa, D. V. O., Portilho-Ramos, R. P., Barbosa, C. F., and Toledo, F. A. L.: Planktonic foraminifera in the sediment of a western boundary upwelling system off Cabo Frio, Brazil, Mar. Micropaleontol., 106, 55–68, https://doi.org/10.1016/j.marmicro.2013.12.002, 2014.

Lessa, D., Morard, R., Jonkers, L., Venancio, I. M., Reuter, R., Baumeister, A., Albuquerque, A. L., and Kucera, M.: Distribution of planktonic foraminifera in the subtropical South Atlantic: depth hierarchy of controlling factors, Biogeosciences, 17, 4313–4342, https://doi.org/10.5194/bg-17-4313-2020, 2020.

https://doi.org/10.5194/egusphere-2025-5531
Preprint. Discussion started: 28 November 2025

Little, M., Schneider, R., Kroon, D., Price, B., Bickert, T., and Wefer, G.: Rapid palaeoceanographic changes in the Benguela Upwelling System for the last 160,000 years as indicated by abundances of planktonic foraminifera, Palaeogeogr. Palaeocl., 130, 135–161, https://doi.org/10.1016/S0031-0182(96)00136-8, 1997.

Lončarić, N., Peeters, F. J. C., Kroon, D., and Brummer, G.-J. A.: Oxygen isotope ecology of recent planktic Foraminifera at the central Walvis Ridge (SE Atlantic), Paleoceanography, 21, PA3009, https://doi.org/10.1029/2005PA001207, 2006.

Longhurst, A. R.: Ecological Geography of the Sea, Academic Press, London, 560 pp., 2010.

Lopes, C. and Mix, A. C.: North Pacific paleotemperature and paleoproductivity reconstructions based on diatom species, Paleoceanogr. Paleoclimatol., 33, 703–715, https://doi.org/10.1029/2018PA003352, 2018.

Lopes, C., Mix, A. C., and Abrantes, F.: Environmental controls of diatom species in northeast Pacific sediments, Palaeogeogr. Palaeoclimatol. Palaeoecol., 297, 188–200, https://doi.org/10.1016/j.palaeo.2010.07.029, 2010.

Lumpkin, R. and Garzoli, S.: Interannual to decadal changes in the western South Atlantic's surface circulation, J. Geophys. Res.-Oceans, 116, C01014, https://doi.org/10.1029/2010JC00628 , 2011.

Lutjeharms, J. R. E. and Stockton, P. L.: Kinematics of the upwelling front off southern Africa, in: The Benguela and Comparable Ecosystems, edited by: Payne, A. I. L., Gulland, J. A., and Brink, K. H., S. Afr. J. Mar. Sci., 5, 25–49, doi: 10.2989/025776187784522612, 1987.

Manly, B. F. J.: Randomization and Monte Carlo Methods in Biology, Chapman & Hall, New York, 281 pp., 1991.

Manta, G., Speich, S., Barreiro, M., Trinchin, R., de Mello, C., Laxenaire, R., et al.: Shelf water export at the Brazil–Malvinas Confluence evidenced from combined in situ and satellite observations, Front. Mar. Sci., 9, 857594, https://doi.org/10.3389/fmars.2022.857594, 2022.

McGarigal, K., Stafford, S., and Cushman, S.: Discriminant analysis, in: Multivariate Statistics for Wildlife and Ecology Research, Springer, New York, NY, 129–187, https://doi.org/10.1007/978-1-4612-1288-1_4, 2000.

McGillicuddy, D. J. and Robinson, A. R.: Eddy-induced nutrient supply and new production in the Sargasso Sea, Deep-Sea Res. Pt. I, 44, 1427–1450, https://doi.org/10.1016/S0967-0637(97)00024-1 , 1997.

Michaels, A. F., Olson, D., Sarmiento, J. L., Ammerman, J. W., Fanning, K., Jahnke, R., Knap, A. H., Lipschultz, F., and Prospero, J. M.: Inputs, losses and transformations of nitrogen and phosphorus in the pelagic North Atlantic Ocean, Biogeochemistry, 35, 181–226, https://doi.org/10.1007/BF02179827 , 1996.

Mohtadi, M., Max, L., Hebbeln, D., Baumgart, A., Krück, N., and Jennerjahn, T.: Modern environmental conditions recorded in surface sediment samples off W and SW Indonesia: Planktonic foraminifera and biogenic compounds analyses, Mar. Micropaleontol., 65, 96–112, https://doi.org/10.1016/j.marmicro.2007.06.004, 2007.

https://doi.org/10.5194/egusphere-2025-5531
Preprint. Discussion started: 28 November 2025

Moore, J. K., Doney, S. C., Glover, D. M., and Fung, I. Y.: Iron cycling and nutrient-limitation patterns in surface waters of the world ocean, Deep-Sea Res. Pt. II, 49, 463–507, https://doi.org/10.1016/S0967-0645(01)00109-6 , 2001.

Moore, C. M., Mills, M. M., Arrigo, K. R., Berman-Frank, I., Bopp, L., Boyd, P. W., Galbraith, E. D., Geider, R. J., Guieu, C., Jaccard, S. L., Jickells, T. D., La Roche, J., Lenton, T. M., Mahowald, N. M., Marañón, E., Marinov, I., Moore, J. K., Nakatsuka, T., Oschlies, A., Saito, M. A., Thingstad, T. F., Tsuda, A., and Ulloa, O.: Processes and patterns of oceanic nutrient limitation, Nat. Geosci., 6, 701–710, https://doi.org/10.1038/ngeo1765 , 2013.

Morey, A. E., Mix, A. C., and Pisias, N. G.: Planktonic foraminiferal assemblages preserved in surface sediments correspond to multiple environment variables, Quat. Sci. Rev., 24, 925–950, https://doi.org/10.1016/j.quascirev.2003.09.011, 2005.

Muller-Karger, F. E., Varela, R., Thunell, R., Luerssen, R., Hu, C., and Walsh, J. J.: The importance of continental margins in the global carbon cycle, Geophys. Res. Lett., 32, L01602, https://doi.org/10.1029/2004GL021346, 2005.

Naidu, P. D. and Malmgren, B. A.: A high-resolution record of Late Quaternary upwelling along the Oman Margin, Arabian Sea based on planktonic foraminifera, Paleoceanography, 11, 129–140, https://doi.org/10.1029/95PA03198, 1996.

Nychka, D., Furrer, R., and Sain, S.: fields: Tools for spatial data, R package version 9, available at: https://cran.r-project.org/web/packages/fields/ (last access: 25 October 2023), 2017.

Oksanen, J., Läärä, E., Huttunen, P., and Meriläinen, J.: Maximum likelihood prediction of lake acidity based on sedimented diatoms, J. Veg. Sci., 1, 49–56, https://doi.org/10.2307/3236052, 1990.

Paparazzo, F. E., Bianucci, L., Schloss, I. R., Almandoz, G. O., Solís, M., and Esteves, J. L.: Cross-frontal distribution of inorganic nutrients and chlorophyll-a on the Patagonian continental shelf of Argentina during summer and fall, Rev. Biol. Mar. Oceanogr., 45, 107–119, https://doi.org/10.4067/S0718-19572010000100011 , 2010.

Paparazzo, F. E., Alder, V. A., Schloss, I. R., Bianchi, A., and Esteves, J. L.: Spatial and temporal trends in the distribution of macronutrients in surface waters of the Drake Passage, Ecol. Austral, 26, 27–39, DOI:10.25260/EA.16.26.2.0.142, 2016.

Pebesma, E. J.: Multivariable geostatistics in S: the gstat package, Comput. Geosci., 30, 683–691, https://doi.org/10.1016/j.cageo.2004.03.012, 2004.

Pebesma, E. J. and Bivand, R. S.: S classes and methods for spatial data: the sp package, R News, 5, 9–13, 2005.

Pereira, L. S., Arz, H. W., Pätzold, J., and Portilho-Ramos, R. C.: Productivity evolution in the South Brazilian Bight during the last 40,000 years, Paleoceanogr. Paleoclimatol., 33, 1339–1356, https://doi.org/10.1029/2018PA003406 , 2018.

https://doi.org/10.5194/egusphere-2025-5531
Preprint. Discussion started: 28 November 2025

Petrick, B. F., McClymont, E. L., Marret, F., and van der Meer, M. T. J.: Changing surface water conditions for the last 500 ka in the Southeast Atlantic: Implications for variable influences of Agulhas leakage and Benguela upwelling, Paleoceanography, 30, 1153–1167, https://doi.org/10.1002/2015PA002787, 2015.

Piola, A. R., and Matano, R. P.: Brazil and Falklands (Malvinas) Currents, in: Encyclopedia of Ocean Sciences, Vol. 1, edited by: Steele, J. H., Thorpe, S. A., and Turekian, K. K., Academic Press, London, 340–349, https://doi.org/10.1006/rwos.2001.0358 , 2001.

Piola, A. R., Matano, R. P., Palma, E. D., Möller, O. O. Jr., and Campos, E. J. D.: The influence of the Plata River discharge on the western South Atlantic shelf, Geophys. Res. Lett., 32, L01603, https://doi.org/10.1029/2004GL021638, 2005.

Piola, A. R., Martínez Avellaneda, N., Guerrero, R. A., Jardón, F. P., Palma, E. D., and Romero, S. I.: Malvinas-slope water intrusions on the northern Patagonia continental shelf, Ocean Sci., 6, 345–359, https://doi.org/10.5194/os-6-345-2010, 2010.

Pivel, M. A. G., Santarosa, A. C. A., Toledo, F. A. L., and Costa, K. B.: The Holocene onset in the southwestern South Atlantic, Palaeogeogr. Palaeoclimatol. Palaeoecol., 374, 164–172, https://doi.org/10.1016/j.palaeo.2013.01.014, 2013.

Portilho-Ramos, R. da C., Ferreira, F., Calado, L., Frontalini, F., and de Toledo, M. B.: Variability of the upwelling system in the southeastern Brazilian margin for the last 110,000 years, Global Planet. Change, 135, 179–189, https://doi.org/10.1016/j.gloplacha.2015.11.003, 2015.

Prell, W. L.: The stability of low-latitude sea-surface temperatures: an evaluation of the CLIMAP reconstruction with emphasis on the positive SST anomalies, Rep. TR025, U.S. Department of Energy, Washington, D.C., 60 pp., 1985.

Rintoul, S. R. and Wunsch, C.: Mass, heat, oxygen and nutrient fluxes and budgets in the North Atlantic Ocean, Deep-Sea Res., 38, S355–S377, https://doi.org/10.1016/S0198-0149(12)80017-3, 1991.

Roberts, D. R., Bahn, V., Ciuti, S., Boyce, M. S., Elith, J., Guillera-Arroita, G., et al.: Cross-validation strategies for data with temporal, spatial, hierarchical, or phylogenetic structure, Ecography, 40, 913–929, https://doi.org/10.1111/ecog.02881, 2017.

Romero, S. I., Piola, A. R., Charo, M., and Eiras García, C. A. E.: Chlorophyll-a variability off Patagonia based on SeaWiFS data, J. Geophys. Res.-Oceans, 111, C05021, https://doi.org/10.1029/2005JC003244, 2006.

Rosell-Melé, A., Martínez-García, A., and McClymont, E. L.: Persistent warmth across the Benguela upwelling system during the Pliocene epoch, Earth Planet. Sci. Lett., 386, 10–20, https://doi.org/10.1016/j.epsl.2013.10.041, 2014.

Rühs, S., Schwarzkopf, F. U., Speich, S., and Biastoch, A.: Cold vs. warm water route – sources for the upper limb of the Atlantic Meridional Overturning Circulation revisited in a high-resolution ocean model, Ocean Sci., 15, 489–512, https://doi.org/10.5194/os-15-489-2019, 2019.

https://doi.org/10.5194/egusphere-2025-5531
Preprint. Discussion started: 28 November 2025

Saraceno, M., Provost, C., Piola, A. R., Bava, J., and Gagliardini, A.: Brazil–Malvinas frontal system as seen from 9 years of AVHRR data, J. Geophys. Res.-Oceans, 109, C05027, https://doi.org/10.1029/2003JC002127, 2004.

Saraceno, M., Provost, C., and Piola, A. R.: On the relationship between satellite-retrieved surface temperature fronts and chlorophyll a in the western South Atlantic, J. Geophys. Res.-Oceans, 110, C11016, https://doi.org/10.1029/2004JC002736, 2005.

Schiebel, R. and Hemleben, C.: Interannual variability of planktic foraminiferal populations and test flux in the eastern North Atlantic Ocean (JGOFS), Deep-Sea Res. Pt. II, 47, 1809–1852, https://doi.org/10.1016/S0967-0645 (00)00008-6, 2000.

Schiebel, R. and Hemleben, C.: Planktic foraminifers in the modern ocean, Springer, Cham, 1–358, https://doi.org/10.1007/978-3-662-50297-6, 2017.

Schiebel, R., Waniek, J., Bork, M., and Hemleben, C.: Planktic foraminiferal production stimulated by chlorophyll redistribution and entrainment of nutrients, Deep-Sea Res. Pt. I, 48, 721–740, https://doi.org/10.1016/S0967-0637(00)00065-0, 2001.

Schiebel, R., Smart, S. M., Jentzen, A., Jonkers, L., Morard, R., Meilland, J., Michel, E., Coxall, H. K., Hull, P. M., de Garidel-Thoron, T., Aze, T., Quillévéré, F., Ren, H., Sigman, D. M., Vonhof, H. B., Martínez-García, A., Kucera, M., Bijma, J., Spero, H. J., and Haug, G. H.: Advances in planktonic foraminifer research: new perspectives for paleoceanography, Rev. Micropaléontol., 61, 113–138, https://doi.org/10.1016/j.revmic.2018.10.001, 2018.

Schlitzer, R.: Ocean Data View, available at: https://odv.awi.de (last access: 25 October 2023), 2014.

Schmidt, G. A., Annan, J. D., Bartlein, P. J., Cook, B. I., Guilyardi, E., Hargreaves, J. C., Harrison, S. P., Kageyama, M., LeGrande, A. N., Konecky, B., Lovejoy, S., Mann, M. E., Masson-Delmotte, V., Risi, C., Thompson, D., Timmermann, A., Tremblay, L.-B., and Yiou, P.: Using palaeo-climate comparisons to constrain future projections in CMIP5, Clim. Past, 10, 221–250, https://doi.org/10.5194/cp-10-221-2014, 2014.

Siani, G., Colin, C., Michel, E., Carel, M., Richter, T., Kissel, C., and Dewilde, F.: Late Glacial to Holocene terrigenous sediment record in the Northern Patagonian margin: Palaeoclimate implications, Palaeogeogr. Palaeoclimatol. Palaeoecol., 297, 26–36, https://doi.org/10.1016/j.palaeo.2010.07.018 , 2010.

Siccha, M. and Kucera, M.: ForCenS, a curated database of planktonic foraminifera census counts in marine surface sediment samples, Sci. Data, 4, 170109, https://doi.org/10.1038/sdata.2017.109, 2017.

Siegel, D. A., McGillicuddy, D. J., and Fields, E. A.: Mesoscale eddies, satellite altimetry, and new production in the Sargasso Sea, J. Geophys. Res.-Oceans, 104, 13359–13379, https://doi.org/10.1029/1999JC900051, 1999.

Sierro, F., Flores, J., Francés, G., Vázquez, A., Utrilla, R., Zamarreño, I., Erlenkeuser, H., and Bárcena, M.: Orbitally-controlled oscillations in planktic communities and cyclic changes in western Mediterranean

https://doi.org/10.5194/egusphere-2025-5531
Preprint. Discussion started: 28 November 2025

hydrography during the Messinian, Palaeogeogr. Palaeocl, 190, 289–316, https://doi.org/10.1016/S0031-0182(02)00611-9, 2003.

Sigman, D. M., Hain, M. P., and Haug, G. H.: The polar ocean and glacial cycles in atmospheric CO_2 concentration, Nature, 466, 47–55, https://doi.org/10.1038/nature09149, 2010.

Signorini, S. R., García, V. M. T., Piola, A. R., Evangelista, H., McClain, C. R., García, C. A. E., and Mata, M. M.: Further studies on the physical and biogeochemical causes for large interannual changes in the Patagonian shelf spring–summer phytoplankton bloom biomass, NASA Tech. Memo., NASA/TM-2009-214176, NASA Goddard Space Flight Center, Greenbelt, MD, USA, 2009.

Signorini, S. R., Franz, B. A., and McClain, C. R.: Chlorophyll variability in the oligotrophic gyres: mechanisms, seasonality and trends, Front. Mar. Sci., 2, 1, https://doi.org/10.3389/fmars.2015.00001, 2015.

Spindler, M. and Dieckmann, G. S.: Distribution and abundance of the planktic foraminifer Neogloboquadrina pachyderma in sea ice of the Weddell Sea (Antarctica), Polar Biol., 5, 185–191, 1986.

Spindler, M., Hemleben, C., Salomons, J. B., and Smit, L. P.: Feeding behavior of some planktonic foraminifers in laboratory cultures, J. Foraminifer. Res., 14, 237–249, doi:10.2113/gsjfr.14.4.237, 1984.

Storz, D., Schulz, H., Waniek, J. J., Schulz-Bull, D. E., and Kucera, M.: Seasonal and interannual variability of the planktic foraminiferal flux in the vicinity of the Azores Current, Deep-Sea Res. Pt. I, 56, 107–124, https://doi.org/10.1016/j.dsr.2008.07.011, 2009.

Stramma, L. and Peterson, R. G.: The South Atlantic Current, J. Phys. Oceanogr., 20, 846–859, https://doi.org/10.1175/1520-0485(1990)020<0846:TSAC>2.0.CO;2, 1990.

Sverdrup, H. U.: On conditions for the vernal blooming of phytoplankton, Rapp. P.-v. Réun. Cons. Int. Explor. Mer, 18, 287–295, https://doi.org/10.1093/icesjms/18.3.287, 1953.

Talley, L. D.: Shallow, intermediate, and deep overturning components of the global heat budget, J. Phys. Oceanogr., 33, 530–560, https://doi.org/10.1175/1520-0485(2003)033<0530:S IADOC>2.0.CO;2, 2003.

Telford, R. J.: palaeoSig: Significance tests of quantitative palaeoenvironmental reconstructions, R package, available at: https://cran.r-project.org/web/packages/palaeoSig/, 2015.

Telford, R. J. and Birks, H. J. B.: Evaluation of transfer functions in spatially structured environments, Quat. Sci. Rev., 28, 1309–1316, https://doi.org/10.1016/j.quascirev.2008.12.020, 2009.

ter Braak, C. J. F.: Permutation versus bootstrap significance tests in multiple regression and ANOVA, in: Bootstrapping and Related Techniques, edited by: Jöckel, K.-H., Rothe, G., and Sendler, W., Springer, Berlin, Heidelberg, 79–85, doi:10.1007/978-3-642-48850-4_10, 1992.

ter Braak, C. J. F. and Juggins, S.: Weighted averaging partial least squares regression (WA-PLS): an improved method for reconstructing environmental variables from species assemblages, Hydrobiologia, 269/270, 485–502, doi:10.1007/BF00028046 ,1993.

https://doi.org/10.5194/egusphere-2025-5531
Preprint. Discussion started: 28 November 2025

ter Braak, C. J. F. and Šmilauer, P.: CANOCO Reference Manual and User's Guide to Canoco for Windows: Software for Canonical Community Ordination (Version 4.5), Microcomputer Power, Ithaca, NY, 2002.

ter Braak, C. J. F. and Verdonschot, P. F. M.: Canonical correspondence analysis and related multivariate methods in aquatic ecology, Aquat. Sci., 57, 255–289, https://doi.org/10.1007/BF00877430, 1995.

Thiede, J.: Distribution of foraminifera in surface waters of a coastal upwelling area, Nature, 253, 712–714, https://doi.org/10.1038/253712a0, 1975.

Toledo, F. A. L., Costa, K. B., and Pivel, M. A. G.: Salinity changes in the western tropical South Atlantic during the last 30 kyr, Glob. Planet. Change, 57, 383–395, https://doi.org/10.1016/j.gloplacha.2007.01.001, 2007.

Trachsel, M. and Telford, R. J.: Technical note: Estimating unbiased transfer-function performances in spatially structured environments, Clim. Past, 12, 1215–1223, https://doi.org/10.5194/cp-12-1215-2016, 2016.

Ufkes, E. and Kroon, D.: Sensitivity of south-east Atlantic planktonic foraminifera to mid-Pleistocene climate change, Palaeontology, 55, 183–204, https://doi.org/10.1111/j.1475-4983.2011.01119.x, 2012.

Ufkes, E., Jansen, J. H. F., and Schneider, R. R.: Anomalous occurrences of Neogloboquadrina pachyderma (left) in a 420-ky upwelling record from Walvis Ridge (SE Atlantic), Mar. Micropaleontol., 40, 23–42, https://doi.org/10.1016/S0377-8398 (00)00033-4, 2000.

Varma, V., Prange, M., Merkel, U., Kleinen, T., Lohmann, G., Pfeiffer, M., Renssen, H., Wagner, A., Wagner, S., and Schulz, M.: Holocene evolution of the Southern Hemisphere westerly winds in transient simulations with global climate models, Clim. Past, 8, 391–402, https://doi.org/10.5194/cp-8-391-2012, 2012.

Voigt, I., Chiessi, C. M., Prange, M., Mulitza, S., Groeneveld, J., Varma, V., and Henrich, R.: Holocene shifts of the southern westerlies across the South Atlantic, Paleoceanography, 30, 39–51, https://doi.org/10.1002/2014PA002677 , 2015.

Wang, X., Auler, A. S., Edwards, R. L., Cheng, H., Ito, E., Wang, Y., Kong, X., and Solheid, M.: Millennial-scale precipitation changes in southern Brazil over the past 90,000 years, Geophys. Res. Lett., 34, L23701, https://doi.org/10.1029/2007GL031149, 2007.

Williams, R. G. and Follows, M. J.: The Ekman transfer of nutrients and maintenance of new production over the North Atlantic, Deep-Sea Res. Pt. I, 45, 461–489, https://doi.org/10.1016/S0967-0637(97)00094-0 , 1998.